University of Bristol - Explore Bristol Research
General rights

Influence of Ring-Strain and Bond Polarization on the Ring-Expansion of Phosphorus Homocycles

Saurabh S. Chitnis, Rebecca A. Musgrave, Hazel A. Sparkes, Natalie E. Pridmore, Vincent T. Annibale and Ian Manners*

School of Chemistry, University of Bristol, Cantock's Close, Bristol, BS8 1TS, United Kingdom

Abstract: Heterolytic cleavage of homoatomic bonds is a challenge as it requires separation of opposite charges. Even highly strained homoatomic rings (e.g. cyclopropane and cyclobutane) are kinetically stable and do not react with nucleophiles or electrophiles. In contrast, cycloalkanes bearing electron donating/withdrawing substituents on adjacent carbons have polarized C–C bonds and undergo numerous heterolytic ring-opening and expansion reactions. Here we show that upon electrophile activation phosphorus homocycles exhibit analogous reactivity, which is modulated by the amount of ring strain and extent of bond polarization. Neutral rings ($^{t}BuP)_3$, **1**, or ($^{t}BuP)_4$, **2**, show no reactivity towards nitriles but the cyclo-phosphinophosphonium derivative $[(^{t}BuP)_3Me]^+$, $[\textbf{3Me}]^+$, undergoes addition to nitriles giving five-membered P_3CN heterocycles. Due to its lower ring-strain, the analogous four-membered ring, $[(^{t}BuP)_4Me]^+$, $[\textbf{4Me}]^+$, is thermodynamically stable with respect to cycloaddition with nitriles, despite similar P–P bond polarization. We also report the first example of isonitrile insertion into cyclophosphines, which is facile for polarized derivatives $[\textbf{3Me}]^+$ and $[\textbf{4Me}]^+$, but does not proceed for neutral **1** or **2**, despite the calculated exothermicity of the process. Finally, we have assessed the reactions of $[\textbf{4R}]^+$ towards 4-dimethylaminopyridine (*dmap*), which suggest that the site of nucleophilic attack varies with the extent of P–P bond polarization. These results deconvolute the influence of ring-strain and bond-polarization on the chemistry of inorganic homocycles and unlock new synthetic possibilities.

Introduction

Strained rings are an important class of molecules and investigations into their properties have revealed fundamental insights into structure, stereochemistry and bonding.[1] They are also precursors to functional materials via ring-opening polymerization (ROP)[2] and key synthetic intermediates en route to complex molecules by cycloaddition reactions.[3] Prototypical three and four-membered carbon rings **I** and **II** (Scheme 1, top) are highly strained, but nevertheless resist nucleophilic, electrophilic, or dipolar ring opening due to the high barrier for heterolytic fission for non-polar C–C bonds (ca. 1300 kJ mol^{-1} in ethane).[4] In contrast, derivatives functionalized with vicinal donor-acceptor groups (**III** and **IV,** Scheme 1, top) have polarized bonds and, consistent with expectation of a lower barrier for C–C heterolysis, a rich ring-opening and expansion chemistry exists for the archetypal organic frameworks **III** and **IV** that is inaccessible to **I** and **II**. For example, while cyclopropane and cyclobutane are both unreactive towards dipolar substrates, a vast array of cycloaddition reaction have been reported between donor-acceptor functionalized cycloalkanes and 1,2-dipoles (e.g. nitriles,[5,6,7,8] nitrosyls,[9,10] ketones,[11] aldehydes[12]), permitting the rapid assembly of complex four-, five-, and six-membered heterocycles.[3,13] In these reactions, donor-acceptor functionalized strained cycloalkanes behave as masked dipoles whose reactivity is analogous to that of canonical dipoles like the azide anion. For example, the reaction of donor-acceptor cyclopropanes with nitriles (Scheme 1, bottom) to give five-membered C$_4$N frameworks (pyrrolines)[5] parallels the reaction of azides with nitriles to give CN$_4$ frameworks (tetrazoles).[14]

A large number of strained inorganic rings are now also known and in some cases their ROP has led to the development of functional inorganic polymers such as polysiloxanes, polyphosphazenes, polythionylphosphazenes,[15] polymetallocenes,[16] and polysilazanes.[17,18,19,20] However, strained rings featuring *homoatomic* inorganic frameworks – especially heavier analogues of **I-IV** – are rare,[21] and their reaction chemistry is therefore underdeveloped, preventing access to materials and molecules with potentially unique physical and chemical properties. Given that bond polarization is the principle underlying the broad synthetic potential of donor-acceptor functionalized cycloalkanes, it is reasonable to expect that strained inorganic homocycles with polarized bonds should also exhibit a rich ring-opening and ring-expansion chemistry. Understanding this chemistry may reveal strategies for evolving complex inorganic systems from the simple cyclic precursors that result from Wurtz coupling of element halides.

Scheme 1. The dipolar reactivity of donor-acceptor functionalized cycloalkanes.
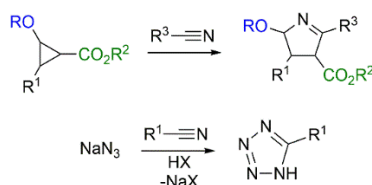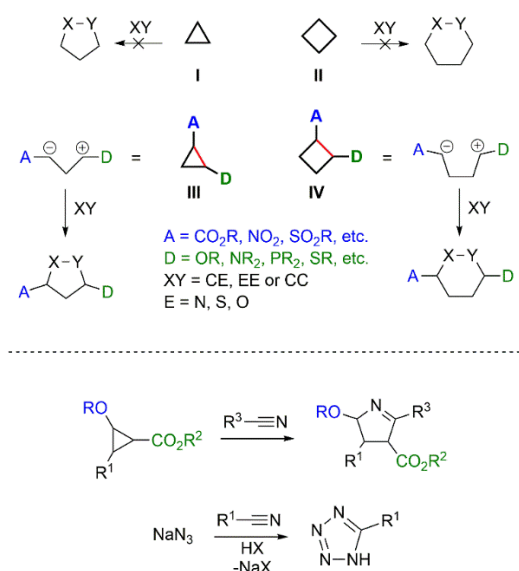
Cyclophosphines represent the most extensively developed class of inorganic homocycles with rings featuring cyclo-P_3, -P_4, -P_5, and -P_6 skeletons having been structurally characterized.[22] Depending upon the size of the substituent at phosphorus, rings with differing sizes can be present simultaneously in solutions. For example, solutions of $(MeP)_n$ contain 1:1:5 ratios of the P_3, P_4, and P_5 homocycles, respectively, at 60 °C.[23] When the bulkier C_4H_9 (^tBu) substituent is employed, stable solutions containing pure ($^tBuP)_3$, **1**, and ($^tBuP)_4$, **2**, can be prepared over a broad temperature range (Figure 1).[24] It is also possible to coordinate a range of electrophiles to one of the phosphine centres in **1** and **2** to access derivatives $[3R]^+$ and $[4R]^+$.[25]
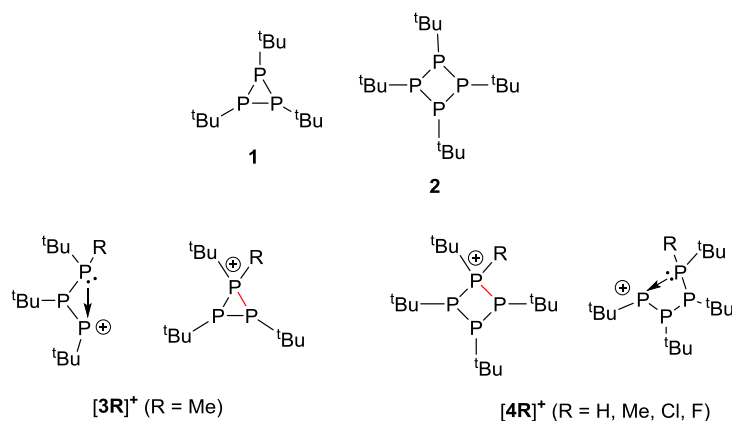
Figure 1. Model compounds for studying the ring-opening and ring-expansion of phosphorus homocycles as a function of ring-strain and bond polarization.

The P–P bonds in phosphino-phosphonium cations, of which [**3R**]$^+$ and [**4R**]$^+$ are a subclass, have been theoretically predicted[26] and experimentally verified[27] by Burford to have lower P–P heterolysis energies compared to neutral diphosphines due to increased polarization of the homoatomic bond. In this regard they are related to the amino-substituted diphosphines compounds extensively studied by Gudat, which also exhibit surprisingly facile P-P bond heterolysis due to resonance-stabilization of the resulting phospheniums.[28] Based on these precedents, we draw the analogy between neutral cyclophosphines (**1**, **2**) and unfunctionalized cycloalkanes (**I**, **II**), which contain nonpolar homoatomic bonds, and between activated cyclophosphines ([**3R**]$^+$, [**4R**]$^+$) containing donor-acceptor bonds and donor-acceptor functionalized cycloalkanes (**III**, **IV**), having polarized homoatomic bonds. This comparison implies a masked dipolar reactivity for cationic cyclophosphines that is kinetically inaccessible to neutral cyclophosphines.

The solution-phase fidelity of ring sizes in **1**, **2**, and their activated derivatives, [**3R**]$^+$ and [**4R**]$^+$, makes them ideal substrates for testing this analogy and, more broadly, for systematically modelling the influence of ring-strain and bond polarization on the ring-opening and ring-expansion chemistry of inorganic homocycles. Here we investigate these factors in the context of cyclophosphine ring-expansion by studying the reactivity of **1**, **2**, [**3Me**]$^+$, and [**4R**]$^+$ (R = H, Me, Cl, F) towards nitriles and isonitriles. Nitriles are prototypical 1,2-dipolar reagents (N – donor, C – acceptor), while isonitriles, due to the simultaneous presence of a lone pair and a vacant p-orbital at the terminal carbon atom in derivatives of R-N=C:, behave as 1,1-dipoles (C – donor, acceptor). We also examine the influence of bond polarization on the ring-opening chemistry for a given framework size in reactions of [**4R**]$^+$ with *dmap*. Our results hint at a rich cycloaddition and ring-opening chemistry for inorganic analogues of donor-acceptor cycloalkanes and provide a theoretical framework within which to predict and interpret this reactivity.

Results and Discussion

Compounds **1** and **2** were prepared as a mixture by reduction of ^{t}BuPCl$_2$ with magnesium, and separated by distillation (Scheme 2).[29] Alkylation of these neutral compounds with methyl triflate yielded salts [**3Me**][OTf] and [**4Me**][OTf].[25] The cation in [**3Me**][OTf] is formed as a racemic mixture of its enantiomers due to the presence of two stereogenic centres in **1**, whereas **2** and derivatives of [**4R**]$^+$ are formed as *meso* compounds. Protonation of **2** with triflic acid gave

4

[**4H**][OTf] and reaction of **2** with a mixture of PCl₅ and Me₃SiOTf gave the salt [**4Cl**][OTf].[25,30,31] The novel salt [**4F**][OTf] was prepared by treatment of a cold (-20 °C) dichloromethane solution containing **2** and Me₃SiOTf with XeF₂ followed by removal of volatile byproducts (Me₃SiF and small amounts of ᵗBuPF₂). The ^{31}P NMR spectrum of [**4F**]⁺ in MeCN showed the expected AM₂X spin system with the quaternary phosphorus centre exhibiting a doublet of triplet of doublets due to $^1J_{PF}$, $^1J_{PP}$, and $^2J_{PP}$ couplings (Figure 2). The ^{19}F NMR spectrum of the salt showed, besides a singlet for the triflate anion, a doublet of triplets with $^1J_{FP}$ and $^2J_{FP}$ coupling constants that matched the values found in the ^{31}P NMR spectrum.

Recrystallization of the crude material from a mixture of CH₂Cl₂/hexane gave [**4F**][OTf] in 71 % isolated yield. Several attempts to obtain single crystals for X-ray crystallographic characterization were unsuccessful yielding only severely twinned crystals that were unsuitable for diffraction. Analysis of a CH₂Cl₂ solution of [**4F**][OTf] by mass spectrometry (electrospray ionization, ESI-MS) revealed the expected M⁺ peak for [**4F**]⁺ at 371.17 m/z, along with peaks corresponding to the fragments [M-ᵗBu]⁺ (315.10 m/z) and [M-2ᵗBu]⁺ (259.04 m/z) from successive loss of alkyl groups. A number of acyclic fluorophosphonium cations are known, and some have found applications as potent Lewis acid catalysts.[32,33] Species [**4F**]⁺ is a rare example of a cyclic fluorophosphonium cation.

**Scheme 2.** Synthesis of compounds **1**, **2**, [**3Me**][OTf], and [**4R**][OTf] (R = H, Me, Cl, F).
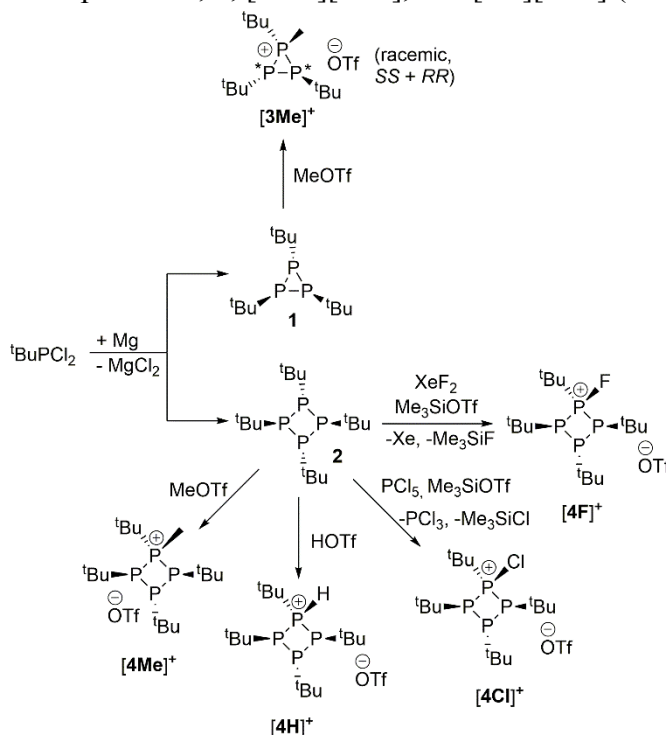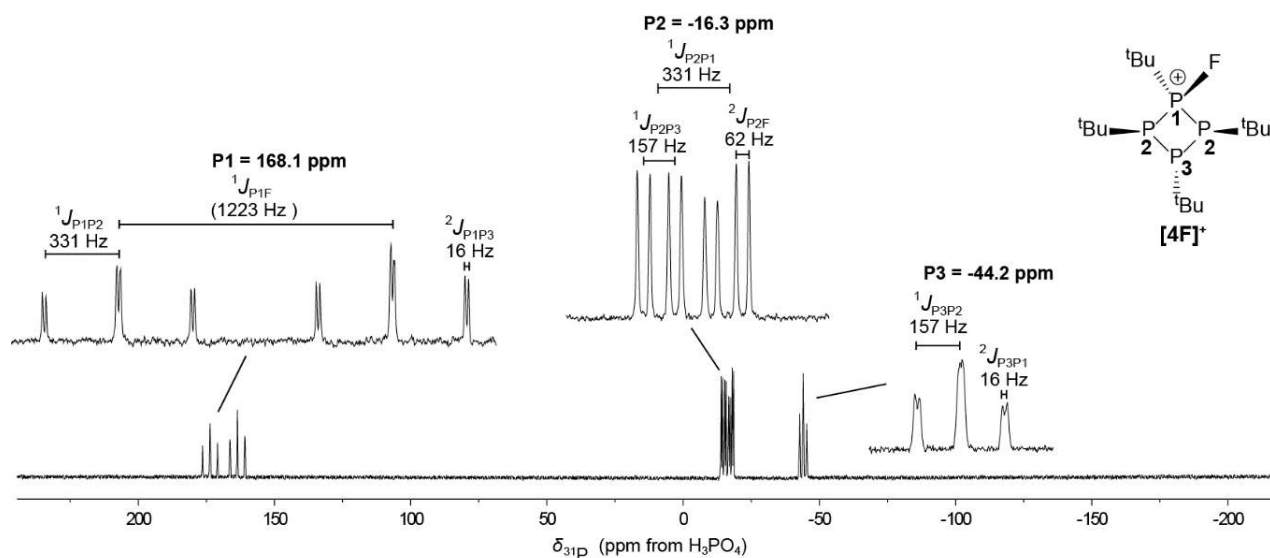
Figure 2. ^{31}P{^{1}H} NMR spectrum (MeCN, 121.66 MHz, 298 K) of [**4F**][OTf].

Ring Strain and Bond Polarization in 1, 2, [3Me]$^+$ and [4Me]$^+$

Calculations of ring-strain in heterocycles containing P-E bonds (E = O, C, S) have been reported previously by Streubel and shown to be valuable in interpreting the reactivity of these ring systems.[34] By contrast, computational assessments of ring-strain in phosphorus *homocycles* are limited to primary cyclophosphines (PH)$_n$ or derivatives with small substituents (e.g. Me).[35,36,37,38,39,40] We have estimated the ring-strain enthalpies in **1**, **2**, [**3Me**]$^+$, and [**4Me**]$^+$ by means of isodesmic reactions shown in Scheme 3 using dispersion-corrected density functional theory (DFT) calculations. These reactions preserve the number and hybridization of each bond, and the molecular charges in the reactants and products.[41] As experimental ring-strain data are not well-established for cyclotriphosphines or cyclotetraphosphines, however, we caution that the values shown in Scheme 3 are only suited for relative comparison rather than as a measure of absolute strain enthalpies.

Comparison of the results for **1** and **2** shows the triphosphorus ring to be nearly 100 kJ mol^{-1} more strained than the tetraphosphorus ring. We consider that the ring-strain in three-membered rings **1** and [**3Me**]$^+$ is comparable, as is the strain in four-membered rings **2** and [**4Me**]$^+$. Therefore expansion reactions of frameworks **1** and [**3Me**]$^+$ should be approximately 100 kJ mol^{-1} more favoured than those of frameworks **2** and [**4Me**]$^+$.

Scheme 3. Isodesmic reactions used to calculate ring-strain enthalpies (kJ mol^{-1}) in **1**, **2**, [**3Me**]$^{+}$ and [**4Me**]$^{+}$.
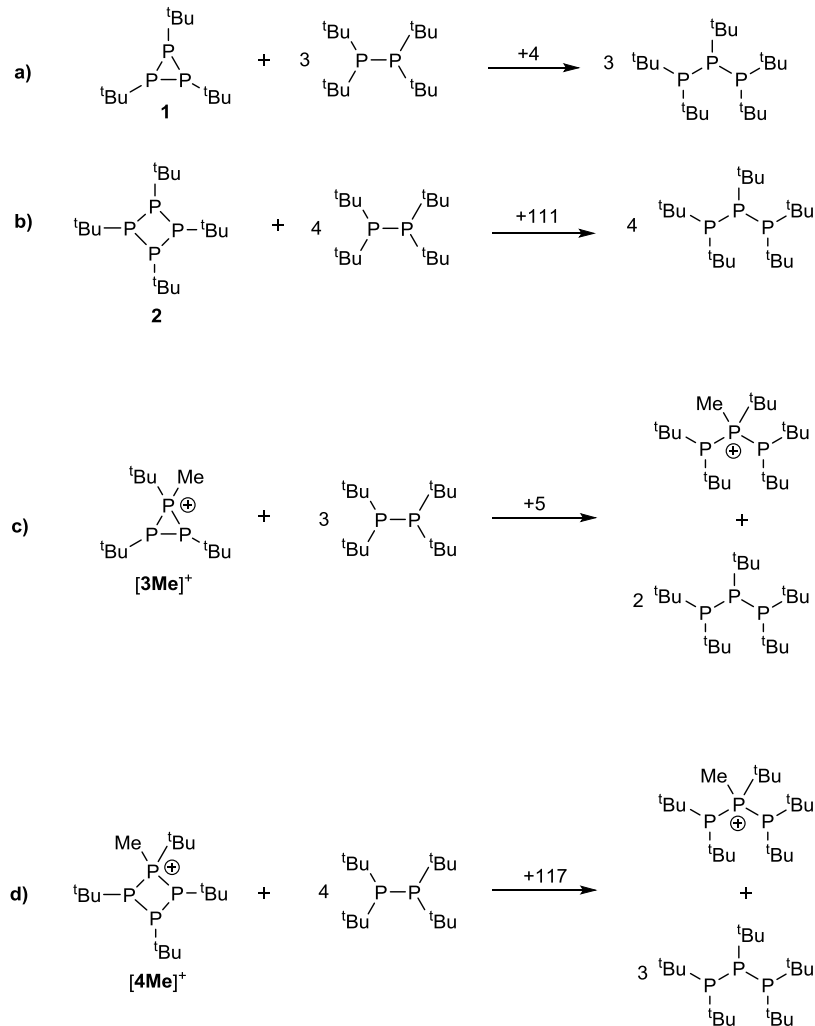
Natural Bond Orbital (NBO) partial charges for the phosphorus atoms in **1**, **2**, [**3Me**]$^{+}$, and [**4Me**]$^{+}$ were also calculated and are given in Figure 3. The difference between the partial charges for adjacent phosphorus atoms provides a measure of bond polarization, with the P-P bond being polarized towards the more positive atom. The partial charges at all phosphorus atoms in **1** or **2** are equal, implying that all P-P bonds in these neutral cyclophosphines are nonpolar. Methylation of the rings leads to drastic increases in the positive charge at the tetravalent phosphorus atoms. For example, the partial charge at P1 increases from +0.26e to +0.82e going from **1** to [**3Me**]$^{+}$ and from +0.27e to +0.91e going from **2** to [**4Me**]$^{+}$. The charges on the remaining trivalent phosphorus atoms in the cations also increase but only marginally, resulting in the overall polarization of P-P bonds towards the tetravalent phosphorus. These

7

values provide a basis for our expectation of dipolar reactivity for [**3Me**]$^+$ and [**4Me**]$^+$, which should be absent in apolar **1** and **2**.
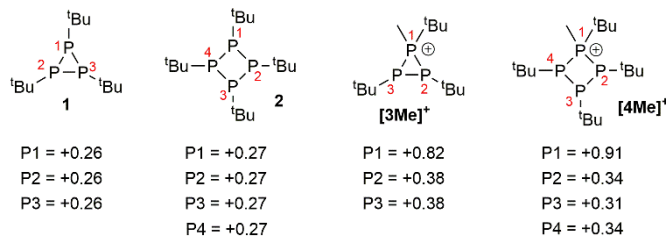
Figure 3. Calculated NBO partial charges for the phosphorus atoms in **1**, **2**, [**3Me**]$^+$ and [**4Me**]$^+$.

Ring-Expansion of Phosphorus Homocycles with Nitriles

Colourless solutions of [**3Me**][OTf] in neat MeCN, EtCN, ^{i}PrCN, ^{t}BuCN or PhCN became pale yellow over 48 h at 25 ^{o}C or upon heating to 80 ^{o}C for 1 h. The ^{31}P NMR spectra of the solutions indicated nearly quantitative formation of new species identified as derivatives of [**5R**][OTf] (R = Me, Et, ^{i}Pr, ^{t}Bu, Ph, Scheme 4a) on the basis of their AMX spin systems (Table S1, Supporting Information). Crystals suitable for diffraction were obtained for [**5Me**][OTf] and [**5Ph**][OTf] and studied by X-ray crystallography. The compounds crystallized in the centrosymmetric space groups *P*-1 and *C*2/*c*, respectively, and the unit cells of each contained two enantiomeric [**5R**]$^+$ cations indicating a racemic mixture of five-membered P$_3$CN heterocycles resulting from the overall addition of racemic [**3Me**]$^+$ across the CN triple bond of the nitriles (Figure 4, Table S3, Supporting Information). In the case of [**5Ph**][OTf] the asymmetric unit included one molecule of Et$_2$O.
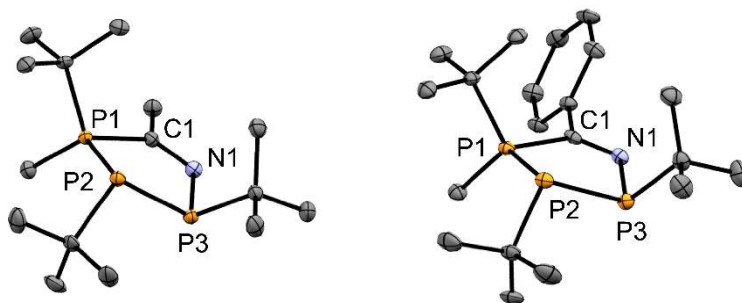
Figure 4. Molecular structure of one of the enantiomers of [**5Me**]$^+$ in the salt [**5Me**][OTf] (left) and [**5Ph**]$^+$ in the salt [**5Ph**][OTf]•Et$_2$O (right). Only one of the two [**5Ph**]$^+$ cations in the asymmetric unit is shown. Hydrogen atoms, triflate anions, and solvent molecules have been omitted for clarity. Thermal ellipsoids are depicted at the 50 % probability level.

Four diastereomers of $[5R]^+$ can be expected, differing by the relative orientation of the ^{t}Bu groups in the P–P–P fragment. In all cases we detected only one diastereomer of $[5R]^+$ by ^{31}P NMR spectroscopy and X-ray crystallography (for R = Me, Ph). DFT calculations for R = Me showed that the observed diastereomer is indeed lowest in energy, with a 27.6 kJ mol^{-1} gap separating it from the next accessible species. This results in a very small K_{eq} (< 0.0001) for the formation of the less stable diastereomer and, consistently, the ^{31}P NMR spectrum of [5Me][OTf] in the 23-80 °C range showed only signals arising from the isolated cation.

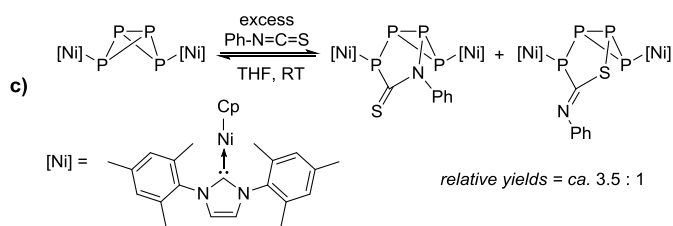The addition of main group π-bonds to C-N multiple bonds is well-established.[42] However, addition of σ-bonds in heavy p-block homocycles to C-N multiple bonds is rare. Passmore et al. reported (Scheme 4b) the cycloaddition of $[S_8]^{2+}$ and $[S_4]^{2+}$ with either $(CN)_2$ to give $[S_3CN]_2[X]_2$ or RCN to give $[S_3CNR][X]$ (X = AsF$_6$, SbF$_6$, Sb$_2$F$_{11}$).[43,44,45,46,47] Very recently, Wolf reported that thiocyanates react with a nickel coordinated P$_4$ cage to give cycloaddition products with either a P$_3$CN or a P$_3$CS framework (Scheme 4).[48] Emphasizing the importance of electrophilic activation in both cases (by molecular charge or coordination to a Lewis acid), there are no reports of S$_8$ or P$_4$ exhibiting analogous cycloaddition with nitriles or thiocyanates. The only other example of a 1-aza-2,3,4-triphospholene framework, as found in $[5R]^+$, was reported by Streubel et al. to result from the reaction of tungsten-bound phosphinidene precursors with nitriles (Scheme 4d), although the products were formed in low yields (< 20 %).[49] Gudat has also shown addition of MeCN to the polarized acyclic P-P bond of a neutral diphosphole in the presence of a tungsten Lewis acid (Scheme 4e).[50]

Scheme 4. Synthesis of [**5R**][OTf] from [**3Me**][OTf] and examples of related reactivity.

a)

[**3Me**]⁺
(racemic)

R-CN
80 °C

[**5R**]⁺
R = Me, Et, ⁱPr, ᵗBu, Ph
(racemic)

b)

$$[S_4]^{2+} + [S_8]^{2+} + 2(CN)_2 \longrightarrow 2$$

$$RCN + 0.24[S_4]^{2+} + 0.24[S_8]^{2+} \longrightarrow$$

c)

excess
Ph-N=C=S
THF, RT

[Ni] + [Ni]

[Ni] =

relative yields = ca. 3.5 : 1

d)

Ph₃PC(H)-CN

120 °C, o-xylene
- Ph(CO₂Me)₂Me₂

e)

MeCN
[W(CO)₄(diene)]

- diene

10
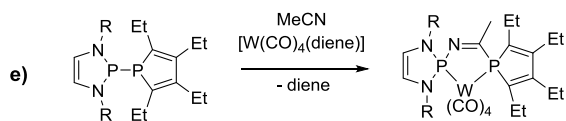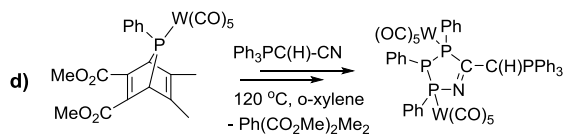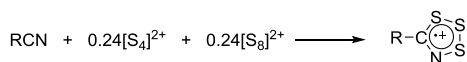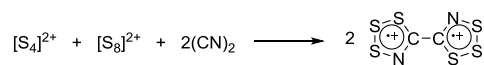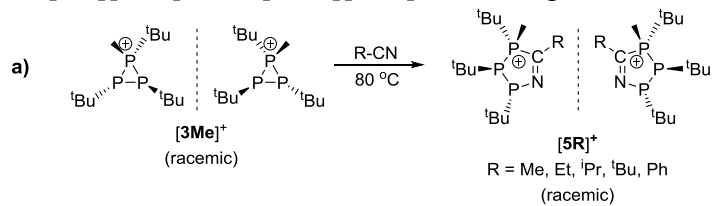
Scheme 5. a) Proposed mechanism for the addition of [**3Me**]$^+$ to nitriles to give [**5Me**]$^+$. b) Ring-opening of [**3Me**]$^+$ with *dmap* to give [**7**]$^+$.
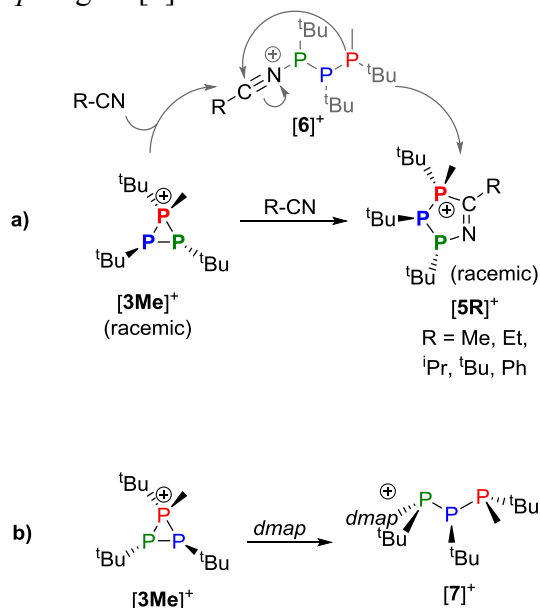
A sequential ring-opening/ring-closing mechanism may be operative in the formation of [**5R**]$^+$, proceeding via the linear intermediate [**6**]$^+$. The closely related linear cation [*dmap*-P(^{t}Bu)P(^{t}Bu)P(^{t}Bu)Me]$^+$ (*dmap* = 4-dimethylaminopyridine), [**7**]$^+$, has been reported by Burford (Scheme 5b).[27b] Activation parameters for the conversion of [**3Me**][OTf] (0.5 M initial concentration) to [**5Me**][OTf] in neat MeCN (19.2 M) were determined by monitoring the reaction using ^{31}P NMR spectroscopy. Logarithmic plots of the concentration of [**3Me**][OTf] against time showed excellent linearity (Figure S1, Supporting Information) giving pseudo first-order rate constants of 0.195 ± 0.005 h^{-1} (313 K), 1.311 ± 0.144 h^{-1} (333 K), 2.819 ± 0.149 h^{-1} (343 K), and 7.067 ± 0.944 h^{-1} (353 K). Eyring analysis (Figure 5) of these values yielded an activation enthalpy, $\Delta H^{\ddagger}$, of 79 ± 2 kJ mol^{-1} and activation entropy, $\Delta S^{\ddagger}$, of -75 ± 5 J mol^{-1} K (Table 1), which is consistent with an associative rate determining step. These values provide scant experimental data for the addition of P-P bonds to polar unsaturated bonds.

Figure 5. Eyring plot for the conversion of [**3Me**][OTf] to [**5Me**][OTf] in neat MeCN.
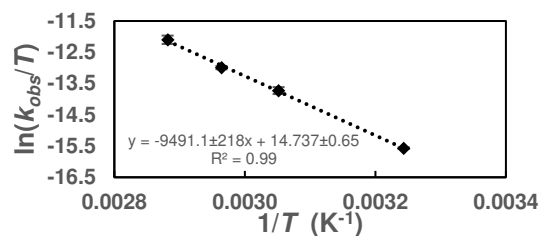
Consideration of solid-state thermodynamics has previously been shown to be important in assessing the stability of polyphosphorus salts.[26] A semi-empirical approach was therefore used to establish the thermodynamic parameters ($\Delta G_{rxn}$, ΔH_{rxn}, and ΔS_{rxn}) for the conversion of [**3Me**][OTf] to [**5Me**][OTf] in neat MeCN. To determine ΔH_{rxn}, the DFT-calculated gas-phase enthalpy for the reaction of [**5Me**]$^+$ and MeCN (ΔH_g = -109 kJ mol^{-1}) was combined in a thermochemical cycle (Figure S2, Supporting Information) with the lattice enthalpies for the two salts ($\Delta H_{lat.}$), and the experimental enthalpy of vaporization of MeCN ($\Delta H_{vap.}$ = 33.25 ± 0.21 kJ mol^{-1}).[51] Lattice enthalpies were extracted from crystallographic unit cell volumes using the method of Jenkins, Passmore and Glasser[52,53] and found to be 397 ± 16 kJ mol^{-1} for [**3Me**][OTf] and 391 ± 16 kJ mol^{-1} for [**5Me**][OTf] (see Experimental). Using these values, the ΔH_{rxn} of -70 ± 22 kJ mol^{-1} was obtained for the conversion of [**3Me**][OTf] to [**5Me**][OTf] in neat MeCN.

Lattice entropies, ΔS_{lat}, were also estimated from the unit cell volume[54] and the values for [**3Me**][OTf] and [**5Me**][OTf] are 752 ± 83 J mol^{-1} K^{-1} and 798 ± 88 J mol^{-1} K^{-1}, respectively. These values were combined with the experimentally known $\Delta S_{vap.}$ for MeCN (111 ± 0.5 J mol^{-1} K^{-1})[55] and the DFT-calculated entropy change in the gas phase, ΔS_g (195 J mol^{-1} K^{-1}), to yield ΔS_{rxn} as -130 ± 121 J mol^{-1} K^{-1} (Figure S2, Supporting Information). From these enthalpy and entropy values, we estimate a relatively small ΔG_{rxn} value of -31 ± 42 kJ mol^{-1} (Table 1) for the formation of [**5Me**][OTf].

Table 1. Activation and standard thermodynamic parameters for the reaction of [**3Me**][OTf] with MeCN to give [**5Me**][OTf].

Parameter	Value
$\Delta H^{\ddagger}$ (kJ mol^{-1})	$+79 \pm 2$
$\Delta S^{\ddagger}$ (J mol^{-1} K^{-1})	-75 ± 5
$\Delta G^{\ddagger}$ (kJ mol^{-1})	$+101 \pm 3$
ΔH_{rxn} (kJ mol^{-1})	-70 ± 22
ΔS_{rxn} (J mol^{-1} K^{-1})	-130 ± 121
ΔG_{rxn} (kJ mol^{-1})	-31 ± 42

Scheme 6. Calculated Gibbs energies (ΔG_{rxn}, 298 K, kJ mol^{-1}) for the addition of MeCN to **1**, **2**, [**3Me**]$^{+}$ and [**4Me**]$^{+}$ in the gas phase.
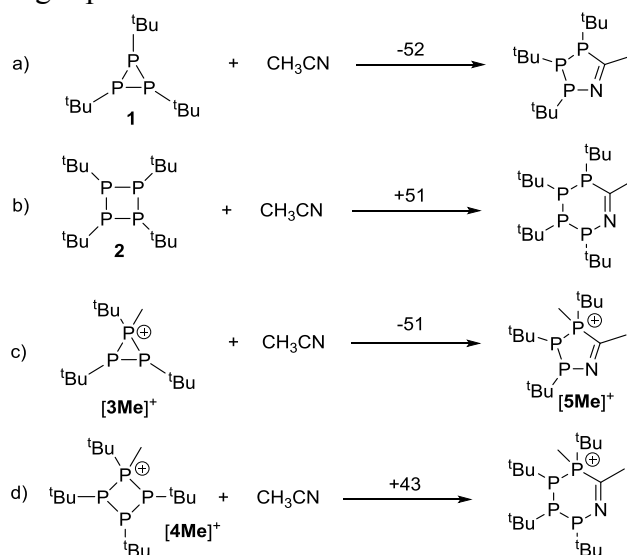
No reaction was observed when **1** was heated to 80 °C in neat MeCN or PhCN for 20 h. Calculated Gibbs energy values (Scheme 6)[56] reveal that addition of MeCN to **1** (-52 kJ mol^{-1}) and [**3Me**]$^{+}$ (-51 kJ mol^{-1}) is equally favourable, and the absence of any reaction between **1** and nitriles may therefore be attributed to a high kinetic barrier. No reaction occurred when either **2** or [**4Me**][OTf] were heated to 80 °C in MeCN or PhCN for 20 h. The calculated ΔG_{rxn} values for the addition of MeCN to **2** and [**4Me**]$^{+}$ are +51 kJ mol^{-1} and +43 kJ mol^{-1}, respectively, and in agreement with the observed lack of reactivity.

Ring-Expansion of Phosphorus Homocycles with Isonitriles

No reaction was detected between **1** or **2** and excess isopropyl isonitrile (^{i}PrNC) either at 25 °C, at 110 °C, or under irradiation with a medium pressure mercury lamp for 24 h (Scheme 7a,b). In contrast, addition of one equivalent of ^{i}PrNC, 2,6-Me$_2$Ph-NC (ArNC) or 1-pentyl isonitrile (PentNC) to clear solutions of [**3Me**][OTf] in CD$_2$Cl$_2$ immediately yielded bright yellow solutions. ^{31}P NMR assays of these reaction mixtures after 2 h showed new resonances exhibiting AMX spin systems in each case and no resonances associated with [**3Me**]$^+$, indicating complete conversion of starting materials to new species [**8R**]$^+$ (Scheme 7c, Table S2, Supporting Information). Crystals obtained from the reaction of [**3Me**][OTf] with ^{i}PrNC unambiguously showed the product to be [**8^{i}Pr**][OTf], where the cation is a four-membered P$_3$C ring with an exocyclic imine at the carbon (Figure 6, left).

Scheme 7. Reactions of **1**, **2**, [**3Me**]$^+$, and [**4Me**]$^+$ with isonitriles.

14
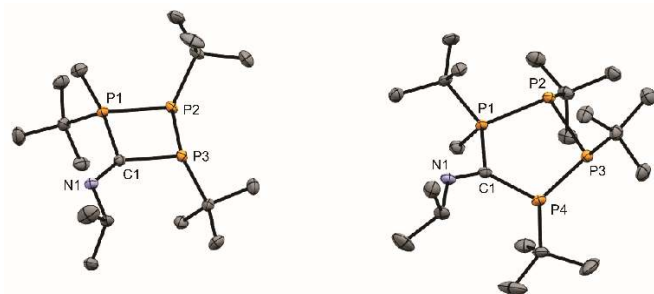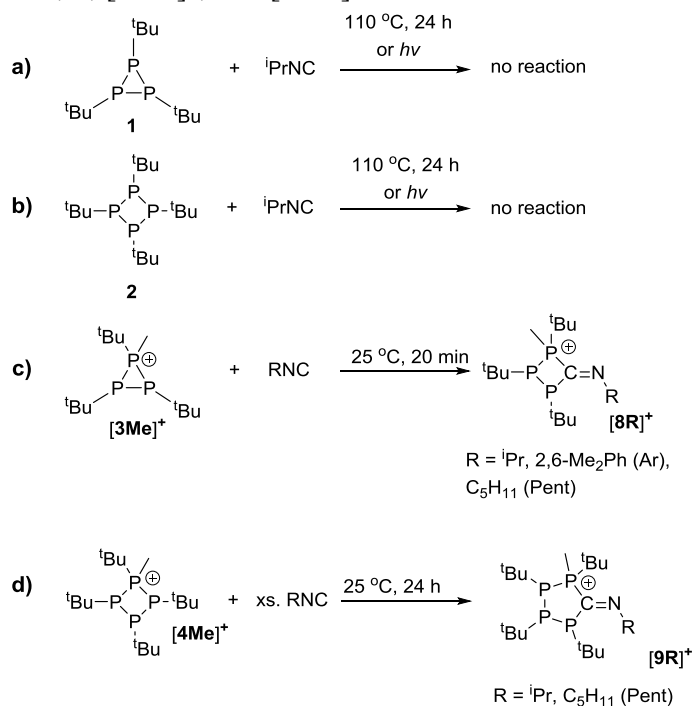
Figure 6. Molecular structure of one of the enantiomers of [**8ⁱPr**]⁺ in [**8ⁱPr**][OTf] (left) and [**9ⁱPr**]⁺ in [**9ⁱPr**][OTf] (right). Hydrogen atoms and triflate anions have been omitted for clarity. Thermal ellipsoids are depicted at the 50 % probability level.

Scheme 8. Proposed mechanism for the formation of [**8R**]⁺ from the reaction of isonitriles with [**3Me**]⁺ (top). Eight diastereomers possible from addition of isonitriles to [**3Me**]⁺ (bottom).
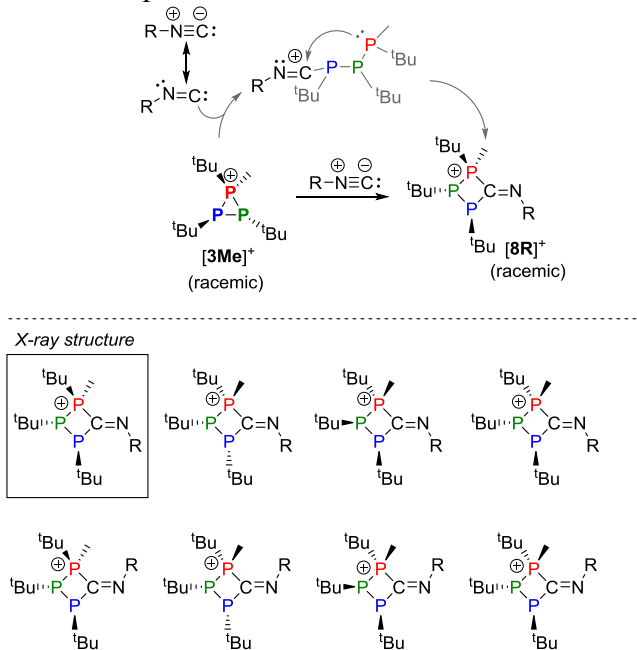
Formation of [**8R**]⁺ from the addition of an isonitrile to [**3Me**]⁺ may occur by a stepwise ring-opening/ring-closing mechanism mechanism (Scheme 8, top). The presence of three stereocentres (P atoms) in [**8R**]⁺ permits four diastereomers, in addition to which, due to the possibility of a *cis* or *trans* arrangement of the imine, an additional four diastereomers are also possible (Scheme 8, bottom). The ³¹P NMR spectrum of the crude reaction mixture containing [**3Me**][OTf] and ⁱPrNC shows three AMX spin systems (Figure S5, Supporting Information). The major AMX spin system (93% by integration) was unambiguously linked to the material isolated upon recrystallization (*trans* arrangement of imine) and the associated ³¹P NMR resonances were the only ones observed upon redissolving the crystals. The two minor components (collectively 7%), are tentatively ascribed to two out of the remaining seven diastereomers, although their formation in small quantities has thus far prevented isolation and structural characterization. In particular, one of the minor AMX spin systems is present in only 1% overall yield. In contrast, the reaction mixture containing [**3Me**][OTf] and the bulkier isonitrile ArNC exhibited only one AMX spin system in its ³¹P NMR spectrum, evidencing the

presence of a single diastereomer of [**8Ar**]⁺ and therefore a course of reactivity that is sensitive to steric bulk at nitrogen.

The reaction of ⁱPrNC with [**4Me**][OTf] was sluggish and showed 65 % consumption of starting materials upon heating to 40 °C for 7 days. When a three-fold excess of the isonitrile was employed, quantitative conversion of [**4Me**][OTf] to [**9ⁱPr**][OTf] was observed within 24 h at 25 °C and no reversal of the reaction was observed upon removal of the excess isonitrile under vacuum (Scheme 7d). The ^{31}P NMR spectrum of [**9ⁱPr**]⁺ showed a fully resolved AGMX spin system with three large $^1J_{PP}$ coupling constants (Figure S6, Supporting Information) confirming the P–P–P–P connectivity. Crystals suitable for diffraction were obtained from a saturated solution in 1:1 MeCN:Et₂O at -30 °C and confirmed the P₄C connectivity for the cation in [**9ⁱPr**][OTf] (Figure 6, right).

The addition of isonitriles to inorganic homocycles has very limited precedence.[57] Weidenbruch reported the oxidative-addition of isonitriles into the Si–Si bonds of cyclotrisilanes and the Ge–Ge bonds of cyclotrigermanes to give ring-expansion products with a Si₃C or Ge₃C framework.[58,59] Sekiguchi and Scheschkewitz have reported the analogous oxidative addition of isonitriles to cyclotrisilenes.[60] Insertion of isonitriles into cyclophosphines has not been reported previously, but Hey-Hawkins recently discovered that the *acyclic* tetraphosphorus dianion in Li₂[P₄(Mes)₄] (Mes = 2,4,6-Me₃Ph) undergoes an unexpected reaction with cyclohexyl isonitrile (C₆H₁₁NC) to give the P₄C heterocycle, (P₄Mes₄)=N-C₆H₁₁, which is a neutral analogue of [**9ⁱPr**]⁺, in 30-60 % yield.[61] In a related case, Streubel has reported the analogous insertion of ᵗBuNC into the tungsten pentacarbonyl activated P-P bond of a four-membered P₂CN heterocycle.[62]

We attempted to determine the activation parameters for isonitrile insertion into [**3Me**]⁺ or [**4Me**]⁺ but these efforts were thwarted by the very rapid (< 5 minutes) conversion of starting materials to products under pseudo-first order conditions (10-fold excess of ⁱPrNC) at room temperature. Similarly, attempts to study reaction kinetics at low temperatures were frustrated by the high crystallinity of the ionic reactants and products, which led to visible precipitation of solids at concentrations required for NMR assays. Standard thermodynamic parameters for the reaction of [**3Me**][OTf] and [**4Me**][OTf] with ⁱPrNC could nevertheless be determined using the volume-based-thermodynamics approach described earlier (see Table 2 and Figure S3 and S4, Supporting Information). Values of ΔH$_{vap}$ and ΔS$_{vap}$ are not known for ⁱPrNC and these were

estimated as 31 ± 3 kJ mol^{-1} and 88 ± 8 J mol^{-1} K^{-1}, respectively, from Trouton's rule (ΔS at boiling point = 88 J mol^{-1} K^{-1})[63] by using the known boiling point of ^{i}PrNC (86 °C).[64]

Table 2. Standard thermodynamic parameters for the reaction of [**3Me**][OTf] and [**4Me**][OTf] with ^{i}PrNC to give [**8^{i}Pr**][OTf] and [**9^{i}Pr**][OTf], respectively.

	[**8^{i}Pr**][OTf]	[**9^{i}Pr**][OTf]
ΔH_{rxn}(kJ mol^{-1})	-106 ± 22	-39 ± 21
ΔS_{rxn}(J mol^{-1} K^{-1})	-246 ± 129	-251 ± 155
ΔG_{rxn}(kJ mol^{-1})	-33 ± 44	+36 ± 51

The enthalpy values show that formation of [**8^{i}Pr**][OTf] is more exothermic than formation of [**9^{i}Pr**][OTf]. The ΔG_{rxn} value for the latter is positive, but no evidence of [**4Me**][OTf] or ^{i}PrNC was detected in solutions of [**9^{i}Pr**][OTf] over 48 h at 25 °C. However, heating a solution of the salt to 80 °C for 20 minutes and then cooling to 25 °C resulted in 95 % retro-addition to [**4Me**][OTf], ^{i}PrNC, and some insoluble material (presumably from polymerization of ^{i}PrNC), suggesting that [**9^{i}Pr**][OTf] is only kinetically stable at 25 °C. In contrast, the ^{31}P NMR spectrum of a solution of [**8^{i}Pr**][OTf] heated to 80 °C for 1 h exhibited no retro-addition to [**3Me**]$^+$ and ^{i}PrNC, confirming the greater thermodynamic stability of [**8^{i}Pr**]$^+$ compared to [**9^{i}Pr**]$^+$.

The reaction of ^{i}PrNC with the remaining derivatives of [**4R**]$^+$ gave varying results depending upon the identity of R. Addition of ^{i}PrNC to [**4H**]$^+$ led to rapid (< 5 minutes) and nearly quantitative deprotonation of the cation to yield neutral **2** (Scheme 9a). The ^{31}P NMR spectrum of the reaction showed a broad resonance for **2**, suggesting an equilibrium between [**2H**]$^+$ and **2** that is mediated by ^{i}PrNC (Figure 7a).

Scheme 9. Products detected by ^{31}P NMR spectroscopy in reactions of [**4H**]$^+$, [**4Cl**]$^+$, and [**4F**]$^+$ with ^{i}PrNC.
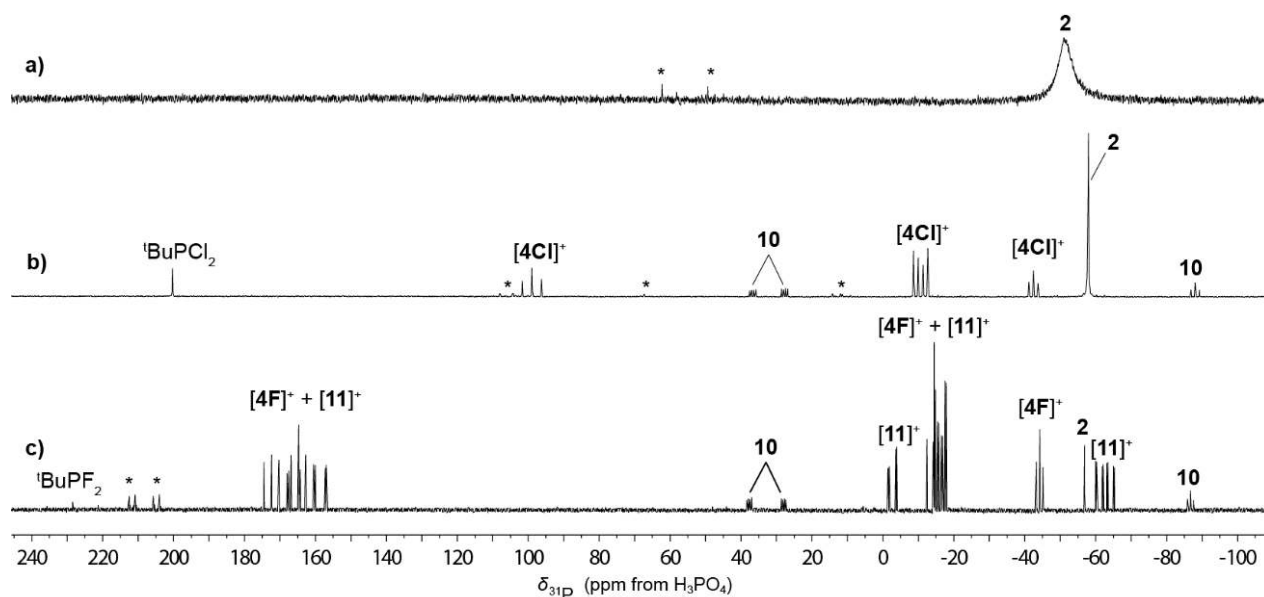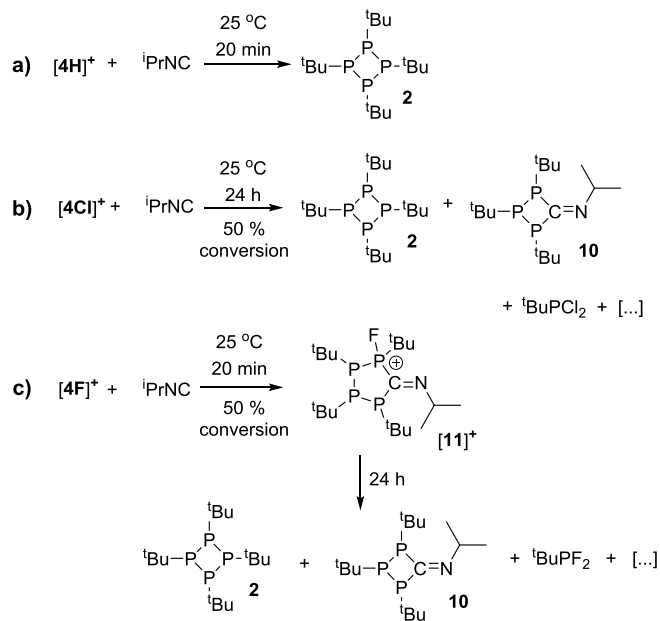
Figure 7. $^{31}P\{^1H\}$ NMR spectra (CH$_2$Cl$_2$, 121.66 MHz, 298 K) of reaction mixtures containing equimolar amounts of ^{i}PrNC and a) [**2H**][OTf], b) [**2Cl**][OTf], and c) [**2F**][OTf]. Asterisks denote unidentified resonances.

The reaction of ^{i}PrNC with one equivalent of [**4Cl**][OTf] stopped after 50 % conversion by ^{31}P NMR spectroscopy (Figure 7b) and yielded a mixture of three phosphorus containing products, of which none exhibited the AGMX spin system expected for the isonitrile insertion product. Two of the products were definitively identified as ^{t}BuPCl$_2$ ($\delta^{31}P$ = 200.3 ppm) and **2**, whereas the third is tentatively assigned to (^{t}BuP)$_3$C=N(^{i}Pr), **10** (Scheme 9b), on the basis of its ABX spin system ($\delta^{31}P$ = 36.7 ppm, 27.7 ppm, and -88.0 ppm) and the associated coupling constants ($^1J_{PP}$ =

18

141 Hz, 142 Hz and $^2J_{PP}$ = 70 Hz). This assignment is also bolstered by comparison with the reported ^{31}P NMR spectrum of (^{t}BuP)$_3$C=O, which shows an A$_2$X spin system with different chemical shifts but similar coupling constants (δ^{31}P = 91.4 ppm – A, -97.6 ppm – X, $^1J_{PP}$ = 164 Hz).[65] The ABX spin system of **10** is of lower symmetry than the A$_2$X spin systems of (^{t}BuP)$_3$C=O because the bent C=N–R fragment of the former belongs to the C_s point group whereas the linear C=O fragment of the latter exhibits $C_{\infty v}$ symmetry. Consistent with evidence from NMR spectroscopy, analysis of the reaction mixture by ESI-MS also showed a peak at 334.19 m/z corresponding to [**10** + H]$^+$. Formation of ^{t}BuPCl$_2$, **2**, and **10** occurs in a 1:2.5:1 ratio and indicates a complex reaction pathway (*vide infra*).

A ^{31}P NMR spectrum of the reaction mixture containing equimolar amounts of ^{i}PrNC and [**4F**][OTf] (Scheme 9c) showed signals due to unreacted [**4F**]$^+$, **10**, ^{t}BuPF$_2$ (δ^{31}P = 228.0 ppm, δ^{19}F = -109.8 ppm, $^1J_{PF}$ = 1180 Hz),[66] **2**, [**11**]$^+$, and one unidentified set of resonances (Figure 7c). The identity of [**11**]$^+$ was established on the basis of its AGMX spin system, the most telling feature of which was the 16-line pattern for the quaternary phosphorus center due to coupling to one fluorine ($^1J_{PF}$ = 1201 Hz) and three unique phosphorus environments ($^1J_{PP}$ = 513 Hz, $^2J_{PP}$ = 13 Hz, $^3J_{PP}$ = 63 Hz). A ^{19}F NMR assay showed the expected eight-line pattern ($^1J_{PF}$ = 1201 Hz, $^2J_{PP}$ = 48 Hz, $^3J_{PP}$ = 16 Hz). Over the course of 24 h signals due to **10**, ^{t}BuPF$_2$ and the unidentified species increased in intensity at the expense of those due to [**11**]$^+$, and no further change was observed upon depletion of the signals for [**11**]$^+$ (Figure S7, Supporting Information) At the end of the reaction, a substantial amount of [**4F**]$^+$ (ca. 50 % by integration) remained in the reaction mixture.

Scheme 10. Calculated Gibbs energies (ΔG_{rxn}) for the addition of ^{i}PrNC to **1**, **2**, [**3Me**]$^+$, and [**4R**]$^+$. All values given in kJ mol^{-1} at 298 K in the gas phase.
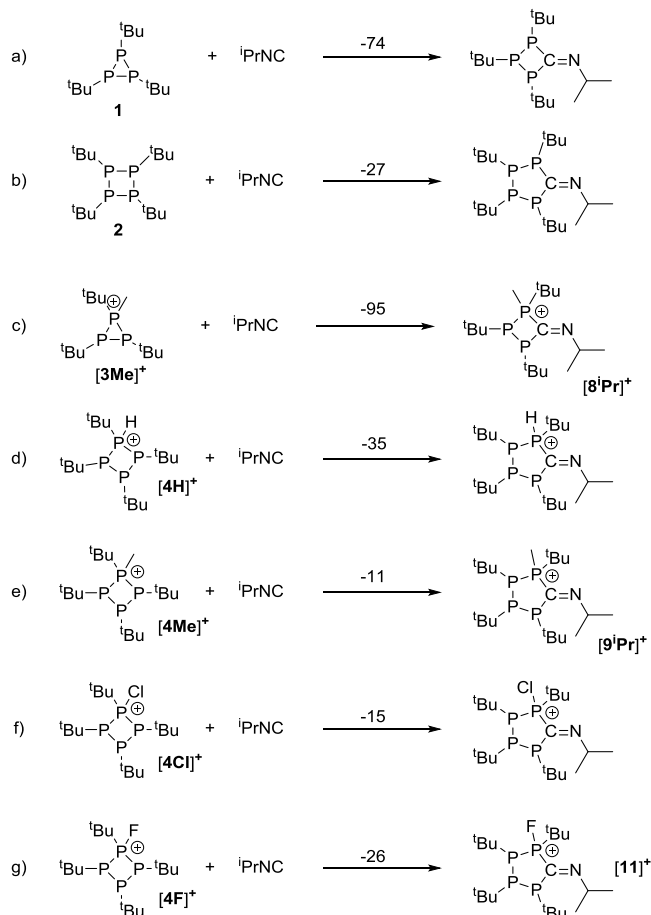
These results are consistent with the initial formation of [**11**]$^+$ and its subsequent decomposition by reaction with a second equivalent of ^{i}PrNC to give a mixture of **10**, ^{t}BuPF$_2$, and the unidentified product. Upon addition of a four-fold excess of ^{i}PrNC to the reaction mixture, the ^{31}P NMR spectrum showed > 90 % conversion of starting material to a mixture of ^{t}BuPF$_2$, **10**, [**11**]$^+$, **2** and the unidentified product but separation of these species could not be effected. However, the spectrum was successfully deconvoluted using iterative lineshape simulation, enabling extraction of chemical shifts and coupling constants for the unisolated compounds **10** and [**11**][OTf] (Figure S8 and Table S2, Supporting Information).

The DFT-calculated[56] ΔG_{rxn} values for insertions of ^{i}PrNC into **1** (-74 kJ mol^{-1}), **2** (-27 kJ mol^{-1}), [**3Me**]$^+$ (-95 kJ mol^{-1}) and [**4Me**]$^+$ (-11 kJ mol^{-1}) are all thermodynamically favourable, albeit to varying degrees (Scheme 10a-d). The different values for three and four-membered rings reflect the relative ring-strain within the respective frameworks. Highlighting the importance of electrophilic activation, however, is the absence of a reaction between **1** or **2** and ^{i}PrNC, whereas [**3Me**]$^+$ and [**4Me**]$^+$ both react to give the corresponding insertion products.

20

Absence of a reaction involving **1** is particularly noteworthy because compound **10**, the anticipated product from the addition of ^{i}PrNC to **1**, was found to be stable in toluene at 120 °C for at least 7 days. Given with the thermodynamic spontaneity calculated for the reactions in Scheme 10 (a, b), we infer the existence of kinetic barriers that prevent formation of insertion products from the neutral rings. These barriers are evidently lowered for the formation of [**8^{i}Pr**]$^+$ and [**9^{i}Pr**]$^+$ from the cationic rings.

Reactions of [4R]$^+$ (R = H, Me, Cl, F) with *dmap*

As shown in the preceding sections, the ring-expansion chemistry of cyclophosphines is modulated by strain and bond polarization. We next considered the influence of these features on the *ring-opening* chemistry of cyclophosphines. Burford has shown previously that [**3Me**]$^+$ is ring-opened to give [**7**]$^+$ in the presence of *dmap* (Scheme 5b), but the analogous ring-opening does not proceed for [**4Me**]$^+$, presumably due to the lower strain in the latter.[27b] Here we isolate the influence of bond polarization on the ring-opening of cyclophosphines by investigating the reactivity of tetraphosphorus frameworks [**4R**]$^+$ (R = H, Cl, F) towards *dmap*. Variations in R lead to differing extents of P-P bond polarization in derivatives of [**4R**]$^+$, as measured using the calculated NBO charges for the phosphorus atoms (Figure S9, Supporting Information).

Scheme 11. Reactions of [**4H**]$^+$, [**4Cl**]$^+$, and [**4F**]$^+$ with *dmap*.
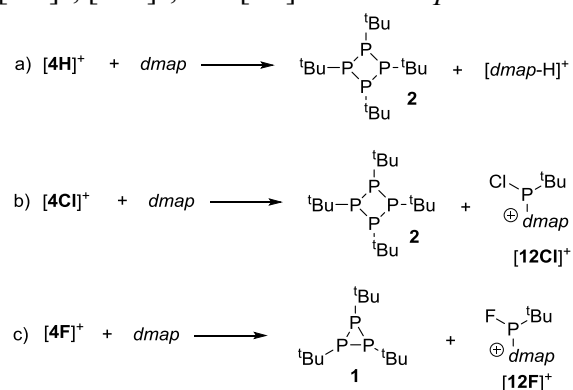
Solutions of [**4R**][OTf] in 1,2-difluorobenzene were treated with one equivalent of *dmap* at 25 °C (or 80 °C in cases where no reaction was detected at room temperature) and assayed by ^{31}P

NMR spectroscopy (Figure S10, Supporting Information). The reaction of *dmap* with [**4H**]$^+$ resulted in rapid (< 10 minutes at 25 °C) and quantitative formation of **2** and [*dmap*-H]$^+$ (Scheme 11a). The reaction of *dmap* with [**4Cl**]$^+$ led to the formation of [*dmap*-P(^{t}Bu)Cl]$^+$ ([**12Cl**]$^+$, δ^{31}P = 159.3 ppm) and **2** in an approximately 1:1 ratio (Scheme 11b). Crystals of [**12Cl**][OTf] were obtained by concentrating the reaction mixture and storing at -35 °C (Figure 8). Lastly, the reaction of *dmap* with [**4F**]$^+$ at 80 °C yielded [*dmap*-P(^{t}Bu)F]$^+$, ([**12F**]$^+$, δ^{31}P = 199.5 ppm, δ^{19}F = -165.9 ppm, $^1J_{PF}$ = 1066 Hz),[67] but, surprisingly, this was accompanied by formation of **1** as the main product with only minor amounts of **2** being detected (Scheme 11c). Equal amounts of ^{t}BuPF$_2$ and [(*dmap*)$_2$P^{t}Bu]$^{2+}$ (δ^{31}P = 139.8 ppm)[68] were also observed, evidencing a substituent redistribution reaction for [**12F**]$^+$.
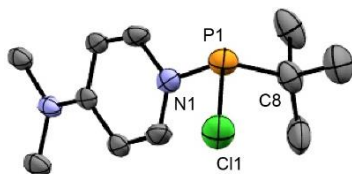
Figure 8. Molecular structure of one enantiomer of [**12Cl**]$^+$ in the salt [**12Cl**][OTf]. Only one of three independent units is shown. Hydrogen atoms and triflate anions have been omitted for clarity. Thermal ellipsoids are depicted at the 50 % probability level.
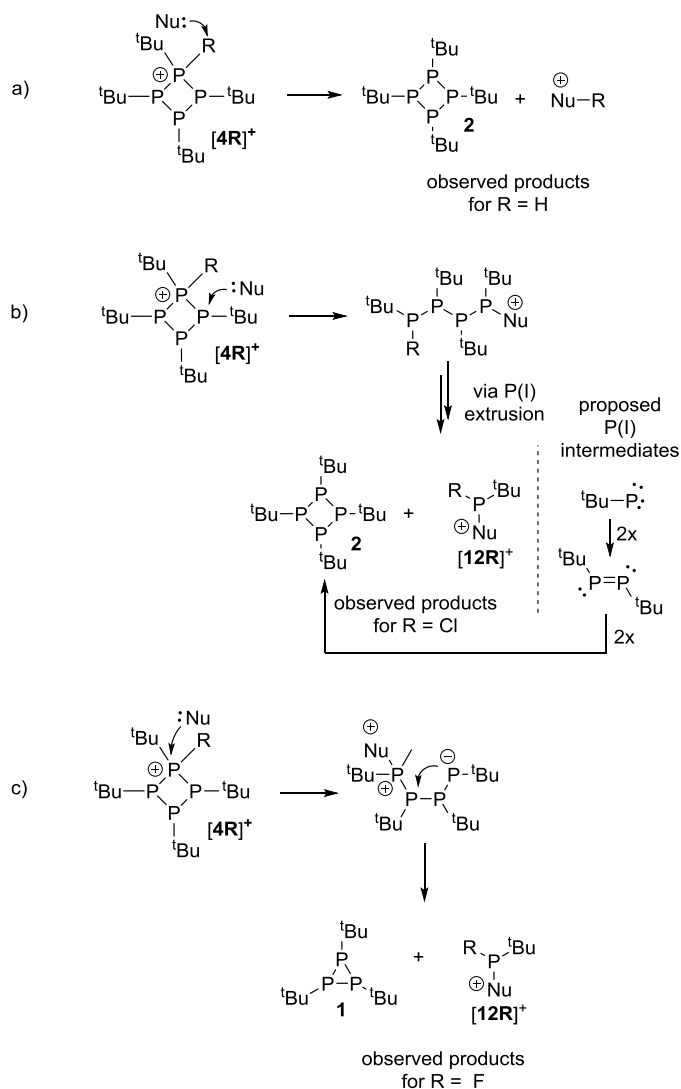
These results map the diverse reaction outcomes for the interaction of nucleophiles with derivatives of [**4R**]$^+$ and may proceed according to the mechanisms shown in Scheme 12. The first route involves exocyclic removal of R$^+$, as exemplified by deprotonation of [**4H**]$^+$ by *dmap* (Scheme 12a). The second proposal involve a stepwise ring opening by nucleophilic attack at either of the two equivalent central phosphorus atoms in derivatives of [**4R**]$^+$, followed by extrusion of a phosphinidene (^{t}BuP), a diphosphene (^{t}BuP=P^{t}Bu), or both, which can undergo oligomerization to produce **2** (Scheme 12 b). The formation of [**12Cl**]$^+$ and **2** in the reaction of *dmap* with [**4Cl**]$^+$ is consistent with this proposal. The final route involves attack at the phosphonium centre effecting a ring opening to give a terminal phosphide. This charge-separated intermediate is expected to be highly unstable and displacement of the phosphonium by intramolecular attack by the terminal phosphide can then yield a neutral contracted ring and a cationic nucleophile-appended phosphine (Scheme 12). Formation of [**12F**]$^+$ and **1** in the reaction of *dmap* and [**4F**]$^+$ is consistent with this course.

Scheme 12. Potential sites of nucleophilic reactivity in derivatives of [**4R**]$^+$.

a) observed products for R = H

b) via P(I) extrusion — proposed P(I) intermediates

observed products for R = Cl

c) observed products for R = F

In the context of these mechanistic models, the site of initial nucleophilic attack in derivatives of [**4R**]$^+$ appears to vary with the extent of electrophilic activation offered by the substituent R. The calculated NBO partial charges at the tetravalent phosphorus (P1 in Figure S9, Supporting Information) increase in the order [**4H**]$^+$ (+0.6 e) < [**4Cl**]$^+$ (+0.9 e) < [**4F**]$^+$ (+1.3 e). The high partial charge at P1 in [**4F**]$^+$ suggests direct nucleophilic attack at the quaternary phosphorus in this cation is plausible, whereas, the partial charge at the quaternary phosphorus in [**4H**]$^+$ is nearly half as positive and therefore exocyclic removal of H$^+$, which is also sterically more accessible, may be rendered a more competitive mode of reactivity. The intermediate polarization at P1 in [**4Cl**]$^+$ is consistent with nucleophilic attack at the less electrophilic P2 or P3 atoms, which could be due to the greater steric accessibility of these trivalent phosphine centers compared to the chlorine substituted tetravalent P1 atom. Crucially, the observation of

23

ring contraction to form **1** and $^tBuPF_2$ in the reaction of [**4F**]$^+$ with *dmap* parallels the detection of the ring contraction product **10** and either $^tBuPF_2$ or $^tBuPCl_2$ in the reaction of [**4F**]$^+$ or [**4Cl**]$^+$ with ^iPrNC, presumably due to nucleophilic attack by the less bulky (compared to *dmap*) ^iPrNC ligand at the highly electrophilic halophosphonium centres in both cases.

Formation and rearrangement of cyclophosphines by extrusion of P(I) intermediates such as phosphinidenes (R–P) or diphosphenes (R–P=P–R) from polyphosphines has been postulated previously but with limited evidence of the extruded species.[25,31,27b,69,70] A generic mechanism showing sequential loss of either phosphinidene or diphosphene units from linear polyphosphines to give cyclophosphiness is shown in Scheme 13a. Cummins has recently shown by means of trapping experiments that a bulky cyclotriphosphine exists in equilibrium with a phosphinidene and a diphosphene.[71] Baudler has proposed an intermolecular σ-bond metathesis process as a means of accessing cyclophosphines of varying sizes (Scheme 13b).[72] As this concerted mechanism does not proceed via unsaturated intermediates, trapping experiments are not expected to yield any products.

Scheme 13. a) Stepwise P(I) extrusion from linear polyphosphines to give cyclophosphines, b) concerted metathesis mechanism for the formation of cyclophosphines from linear polyphosphines, and c) synthesis and thermal decomposition of [**7**]$^+$.
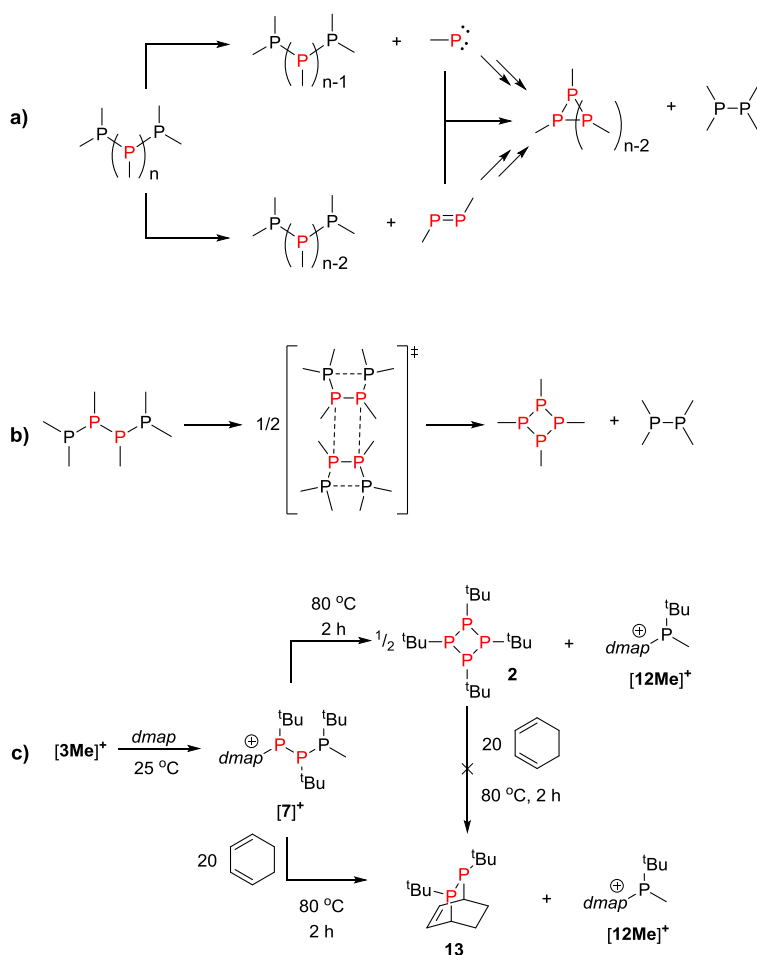
Since formation of **2** in the reaction of [**4Cl**]$^+$ with *dmap* could occur by either of the two mechanisms, we repeated the reaction in the presence of 20 equivalents of 1,3-cyclohexadiene as a potential trapping agent. However, due to the high Lewis acidity of halophosphonium cations, these experiments only showed catalytic polymerization of the diene,[73] which was indicated by formation of intensely coloured solutions of polycyclohexene within seconds of adding 1,3-cyclohexadiene to a mixture of [**4Cl**]$^+$ and *dmap*.[74] To circumvent cation-initiated diene polymerization, we investigated the thermal decomposition of the closely related and isolable cation [**7**]$^+$, which is analogous to the linear intermediate proposed in the reaction of *dmap* with [**4Cl**]$^+$ (Scheme 12b), but less electrophilic due to replacement of a chlorine atom with a CH$_3$ group.

The ^{31}P NMR spectrum of a freshly prepared 1,2-difluorobenzene solution of [**7**][OTf] showed the AMX spin system previously reported for the cation.[27b] Upon heating this solution to 80 °C for 2 h, a yellow colour appeared and a ^{31}P NMR assay showed quantitative conversion to [*dmap*-P(^{t}Bu)Me]$^+$, ([**12Me**]$^+$, δ^{31}P = 108.2 ppm)[75] and **2** (Scheme 13c). Repeating the reaction in

the presence of 20 equivalents of 1,3-cyclohexadiene showed complete conversion to $[\mathbf{12Me}]^+$ and the expected diphosphene trapping product, $\mathbf{13}$ ($\delta^{31}P$ = -13.3 ppm, 4.2 ppm, $^1J_{PP}$ = 264 Hz), with $\mathbf{2}$ being formed in less than <15 % spectroscopic yield (Scheme 13c, see also Figure S12, Supporting Information). The AB spin system observed in the ^{31}P NMR spectrum of $\mathbf{13}$ implies a *trans* configuration of the ^tBu groups about the P-P bond. Consistently, ^1H NMR spectra indicate a C_1 rather than C_s molecular symmetry for the molecule (Figure S13, Supporting Information). On the basis of reported trends in values of $\delta^{31}P$ for *syn-* or *anti*-configured phosphanorbornane derivatives,[76] the more downfield resonance at 4.2 ppm is assigned to the the *syn*-phosphorus centre having the ^tBu group directed toward the alkene functionality. Extraction of the reaction mixture with benzene resulted in enrichment of the NMR signal due to neutral $\mathbf{13}$ and reduction of the signal due to ionic $[\mathbf{12Me}][OTf]$, which exhibits low solubility in nonpolar aromatic solvents. Analysis of this benzene extract by ESI-MS showed a peak at 273.15 m/z assigned to the $[M+O+H]^+$ ion formed by oxidation of $\mathbf{13}$ during sample injection under ambient atmosphere. Control experiments showed no evidence of $\mathbf{13}$ when $\mathbf{2}$ was heated to 80 °C for 24 h in 1,2-difluorobenzene in the presence of a 20-fold excess of 1,3-cyclohexadiene, precluding a retro-dimerization from $\mathbf{2}$ to yield $^tBuP=P^tBu$ and subsequent trapping. We therefore conclude that either diphosphene $^tBuP=P^tBu$ or phosphinidene ^tBuP (which can rapidly dimerize to $^tBuP=P^tBu$) are transiently formed in the thermal decomposition of $[\mathbf{7}]^+$, ruling out a concerted σ-bond metathesis mechanism for the formation of $\mathbf{2}$.

As formation of $[\mathbf{12Me}]^+$ and $\mathbf{11}$ from $[\mathbf{7}]^+$ parallels that of $[\mathbf{12Cl}]^+$ and $\mathbf{2}$ in the reaction of *dmap* with $[\mathbf{4Cl}]^+$, it is plausible that analogous P(I) extrusion processes are operative in both cases. Nevertheless, due to the donor-acceptor nature of the interaction between *dmap* and derivatives of $[\mathbf{4R}]^+$, dynamic equilibria that involve transient ring-opening and closure prior to formation of more stable products cannot be ruled out.

Summary and Conclusions

Species $\mathbf{1}$, $\mathbf{2}$, $[\mathbf{3Me}]^+$ and $[\mathbf{4R}]^+$ represent a model system to study the ring-opening and ring-expansion chemistry of inorganic homocycles. We have computationally assessed the degree of ring-strain in $\mathbf{1}$, $\mathbf{2}$, $[\mathbf{3Me}]^+$ and $[\mathbf{4Me}]^+$ by using isodesmic schemes. Compound $\mathbf{1}$ is more strained than $\mathbf{2}$ but there is no significant difference in the ring-strain between $\mathbf{1}$ and $[\mathbf{3Me}]^+$ or between $\mathbf{2}$ and $[\mathbf{4Me}]^+$. The P-P bonds in the cationic derivatives are strongly polarized towards

the quaternary phosphorus centers with predictions of a masked dipolar reactivity analogous to donor-acceptor cycloalkanes. Consistently, the reaction of [**3Me**]$^+$ with nitriles gave derivatives of [**5R**]$^+$ constituting a rare example of addition between inorganic homocycles and species with CN bonds. The reaction exhibits striking similarities to the reaction of donor-acceptor cyclopropanes with nitriles to give pyrrolines (Scheme 14, top). No reaction was observed between nitriles and **1** even though DFT calculations predict the addition to be as thermodynamically favourable as in the case of [**3Me**]$^+$. Since the ring-strain in the two species is comparable, this discrepancy points to a substantial kinetic barrier for ring-expansion in **1** that is lowered in [**3Me**]$^+$ due to polarization of the homoatomic P-P bond by electrophile coordination. Stronger interactions with nucleophiles on electrostatic grounds also contributes towards an enhanced reactivity for the cationic derivatives relative to neutral species. However, DFT calculations predict the absence of the analogous reaction between nitriles and either **2** or [**4Me**]$^+$ due to the lower ring-strain of the tetraphosphine frameworks, and these predictions were verified experimentally.

We also showed the first example of isonitrile insertion into phosphorus homocycles in reactions involving either [**3Me**]$^+$ or [**4Me**]$^+$, which gave [**8R**]$^+$ and [**9R**]$^+$, respectively, containing a P$_3$C or P$_4$C framework with exocyclic imines. This insertion is analogous to the addition of donor-acceptor cycloalkanes to isonitriles, which yields cycloalkanimines as intermediates en route to more complex products (Scheme 14, middle).[77] No reaction was observed between isonitriles and **1** or **2**, despite predictions from DFT calculations that insertion into these homocycles is thermodynamically viable. Lastly, we studied the reactivity of [**4R**]$^+$ (R = H, Cl, F) with *dmap* and found surprising variations in the observed reaction outcomes that may be explained in part by variations in the initial site of nucleophile attack (Scheme 14, bottom).

Scheme 14. Top: dipolar reactivity of donor-acceptor cyclopropanes and [**3Me**]$^+$ with nitriles (1,2-dipole). Middle: dipolar reactivity of donor-acceptor cyclopropanes and [**3Me**]$^+$ with isonitriles (1,1-dipole). Bottom: reactions of [**4R**]$^+$ with nucleophiles.
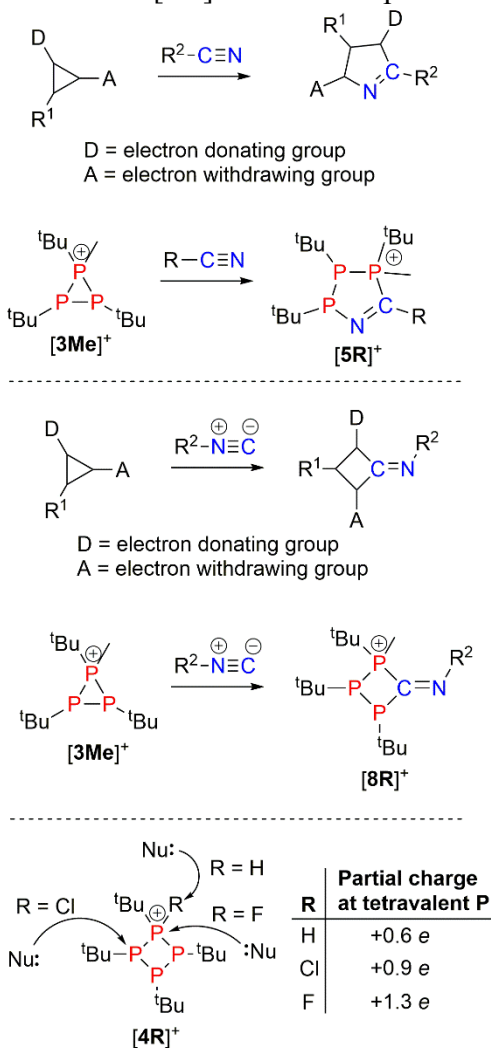
These results show the dipolar nature of the homoatomic bonds in cationic cyclophosphines by analysis of their reactivity towards polar unsaturated substrates. Since the reactivity of charged cyclophosphines [**3Me**]$^+$ and [**4Me**]$^+$ resembles that of donor-accceptor functionalized cycloalkanes, we envision that some of the numerous transformations accessible to the latter should also be viable for the former, offering new synthetic opportunities. We also deconvolute the influence of ring-strain and electrophilic activation on the ring-expansion and ring opening chemistry of phosphorus homocycles: high ring-strain generates a thermodynamic driving force for ring-expansion or opening, and electrophilic activation lowers the kinetic barrier(s) along the reaction coordinate to realize the thermodynamic outcome. Since ring-expansion in small cyclophosphines appears to be only kinetically hindered, transient bond

polarization by added electrophiles could reveal new catalytic routes for accessing complex heterocycles from simple Wurtz coupling products such as **1** and **2**.

Experimental

General Considerations: All manipulations were carried out under an atmosphere of dry and deoxygenated N_2 in a glovebox (H_2O and O_2 < 0.1 ppm) or using standard Schlenk methods. Glassware was predried in an oven at 250 °C for several hours and cooled under dynamic vacuum prior to use. Solvents were dried and deoxygenated using a Grubbs type column and stored over activated 3 Å molecular sieves for a minimum of 24 hours. Compounds **1**,[29] **2**,[29] [**3Me**][OTf],[25] [**4Me**][OTf],[25] [**4H**][OTf],[25] and [**4Cl**][OTf][31] were prepared according to literature routes. All other reagents were obtained at the highest purity from Sigma-Aldrich. Liquids (Me_3SiOTf, PCl_3, 1,3-cyclohexadiene, nitriles, and isonitriles) were distilled prior to use and solids ($^tBuPCl_2$, *dmap*, PCl_5, and XeF_2) were used as received. *Note: Reactions involving XeF_2 should be conducted on small scales (< 5 mmol) in oxidatively resistant solvents (e.g. CH_2Cl_2, MeCN) with measures taken to vent the Xe gas formed.*

NMR spectra were obtained using JEOL ECP 300 (300 MHz), Varian-400 (400 MHz), or Varian NMRS500 (500 MHz) spectrometers at 298 K unless otherwise stated. Deuterated solvents were obtained from Sigma-Aldrich and dried by storage over activated 3 Å molecular sieves for 24 hours. Air sensitive samples were loaded and capped in NMR tubes inside the glovebox and sealed with Teflon tape and Parafilm prior to removal. ^{31}P NMR kinetic experiments were carried out in hermetically sealed J-Young valved NMR tubes with a capillary containing neat PCl_3 as an internal standard.

Synthesis and characterization:

[4F][OTf]: A solution of XeF_2 (250 mg, 1.5 mmol) in 10 mL DCM was cooled to 0 °C and dropwise added to a cooled (-20 °C) solution of **2** (352 mg, 1 mmol) and TMSOTf (444 mg, 2 mmol) in 10 mL DCM. Effervescence was observed and a clear yellow solution was obtained by the end of the addition. After stirring for 10 minutes at -15 °C and subsequently for 30 minutes at ambient temperature, all volatiles were removed under vacuum to obtain a white powder. Unreacted **2** was removed by washing thrice with 2 mL hexanes at room temperature. Recrystallization from a 1:1 mixture of MeCN/Et_2O yielded [**4F**][OTf] as an air and moisture sensitive white powder. Yield: 71%. Elemental analysis with 0.5 eq MeCN (calc./expt.): C − 39.97/40.70, H − 6.99/7.21, N − 1.29/0.92. ^1H NMR (CD_2Cl_2, 400.19 MHz, 298.15 K): δ_H 1.34 (dt, $J = 15.3$ Hz, 1.2 Hz, 9H), 1.47 (d, $J = 21$ Hz, 9H), 1.52 (d, $J = 18$ Hz, 18H). The resonance at 1.47 ppm and 1.52 ppm exhibited significant overlap, 1.95 (s, 1.3H − partial solvent inclusion). ^{13}C NMR (CD_2Cl_2, 75.57 MHz, 298.15 K): δ_C 2.1 (s − partial solvent inclusion), 21.8 (q, $J = 3$ Hz), 27.9 (dt, $J = 16, 5$ Hz), 30.5 (m), 31.5 (m), 41.7 (m), 121.1 (q, $J = 320$ Hz). $^{31}P\{^1H\}$ NMR (CD_2Cl_2, 162.00 MHz, 298.15 K): δ_P -44.2 (td, $J = 157, 16$ Hz, 1P), -16.3 (ddd, $J = 331, 157, 62$ Hz, 2P), 168.1 (dtd, $J = 1223, 331, 16$ Hz, 1P). ^{19}F NMR (CD_2Cl_2, 282.78 MHz, 298.15 K): δ_F -177.50 (dt, $J = 1223, 62$ Hz, 1F), -78.86 (s). ESI-MS: 371.17 m/z, [**4F**]$^+$.

[5Me][OTf]: A colourless solution of [**3Me**][OTf] (428 mg, 1 mmol) in 4 mL MeCN was heated to 80 °C for 2 hours to obtain a bright yellow solution. Analysis of this crude reaction mixture by ^{31}P NMR showed quantitative conversion of starting materials to [**5Me**][OTf]. The reaction mixture was concentrated to 1 mL, layered with Et_2O, and cooled to -30 °C for 3 days to obtain yellow crystalline blocks suitable for X-ray crystallography. The supernatant was decanted and the solids dried under vacuum to yield [**5Me**][OTf] as a yellow powder. Yield: 414 mg, 88 %. Elemental analysis (calc./expt.): C − 40.94/41.06, H − 7.09/7.10, N − 2.98/3.01. ^1H NMR (CDCl$_3$, 499.89 MHz, 298.15 K): δ_H 1.23 (d, $J = 14.2$ Hz, 1H), 1.45 (d, $J = 16.3$ Hz, 9H), 1.49 (d, $J = 18.1$ Hz, 9H) , 2.52 (d, $J = 11.5$ Hz, 3H) 2.70 (t, $J = 5.0$ Hz, 3H). ^{13}C NMR (CDCl$_3$, 125.71 MHz, 298.15 K): δ_C 5.56 (dd, $J = 17.1, 4.1$ Hz), 26.03 (d, $J = 3.9$ Hz) , 26.24 (d, $J = 6.3$ Hz), 27.73 (dd, $J = 13.3, 5.5$ Hz), 31.92 (dt, $J = 14.4, 5.2$ Hz), 34.6-35.1 (m), 35.48 (dd, $J = 30.8, 13.6$ Hz), 120.8 (q, $J = 319$ Hz), 162.81 (d, $J = 10.7$ Hz). $^{31}P\{^1H\}$ NMR (CDCl$_3$, 121.66 MHz,

298.15 K): δ_P -57.03 (dd, J = 421, 262 Hz), 87.94 (dd, J = 421, 30 Hz), 129.61 (dd, J = 262, 31 Hz). ^{19}F NMR (CDCl$_3$, 282.78 MHz, 298.15 K): δ_F -78.80 (s).

[5R][OTf]: These compounds were prepared and characterized in situ in NMR tubes using the procedure for [**5Me**][OTf] on a 0.1 mmol scale and using 0.5 mL of the appropriate nitrile as the solvent (e.g. PhCN for [**5Ph**][OTf]). The ^{31}P NMR data are given in Table S1 (Supporting Information). In the case of [**5Ph**][OTf] a small amount of crystalline material was serendipitously obtained and further characterized by X-ray crystallography.

[8Ar][OTf]: Prepared as per the procedure and on the scale employed for [**8^{i}Pr**][OTf] using 2,6-dimethylphenyl isocyanide (ArNC) instead of ^{i}PrNC. Yield: 397 mg, 71 %. Elemental analysis (calc./expt.): C – 49.37/50.45, H – 7.03/7.13, N – 2.50/2.79. Carbon analysis consistently yielded high results, whereas H and N analysis were consistently close to calculated values. ^{1}H NMR (CD$_2$Cl$_2$, 300.53 MHz, 298.15 K): δ_H 0.90 (d, J = 15.8 Hz, 9H), 1.53 (dt, J = 16.7 Hz, 1.0 Hz, 9H), 1.60 (d, J = 19.2 Hz, 9H), 2.21 (s, 3H), 2.27 (s, 3H), 2.55 (dd, J = 12.5 Hz, 1.3 Hz, 3H), 7.08-7.18 (m, 3H). ^{13}C NMR (CD$_2$Cl$_2$, 125.71 MHz, 298.15 K): δ_C 6.8 (d, J = 18 Hz), 18.8 (d, J = 14 Hz), 19.0 (s), 28.5 (dd, J = 14, 4 Hz), 24.5 (d, J = 3 Hz), 30.7 (ddd, J = 15, 5, 4 Hz), 33.9 (ddd, J = 32, 15, 4 Hz), 37.5 (ddd, J = 20, 11, 2 Hz), 39.9 (ddd, J = 34, 16, 8 Hz),120.9 (q, 319 Hz), 127.1 (s), 128.5 (s), 128.9 (s), 129.7 (s), 147.6 (d, J = 28 Hz), 166.1 (ddd, J = 70, 57, 14 Hz). ^{31}P{^{1}H} NMR (CD$_2$Cl$_2$, 121.66 MHz, 298.15 K): δ_P -54.01 (dd, J = 269.0, 164.5 Hz, 1P), 52.91 (dd, J = 269.1, 39.4 Hz, 1P), 94.71 (dd, J = 164.8, 39.6 Hz, 1P). ^{19}F NMR (CD$_2$Cl$_2$, 282.78 MHz, 298.15 K): δ_F -78.80 (s). ESI-MS: 410.2 m/z [**8Ar**]$^{+}$.

[8^{i}Pr][OTf]: Neat ^{i}PrNC (69 mg, 1 mmol) was added at once to a stirred solution of [**3Me**][OTf] (428 mg, 1 mmol) in 2 mL DCM to yield a reddish brown reaction mixture. Analysis by ^{31}P NMR after 20 minutes revealed complete consumption of starting materials and appearance of three new AMX spin systems in approximately 93:6:1 relative intensities. All volatiles were removed after stirring for an additional hour. The resulting solids were dissolved in a minimum amount of 1,2-difluorobenzene, layered with pentane, and kept at -30 °C for three days to give brown crystalline material that was suitable for X-ray crystallography. The redissolved crystals exhibited a single AMX spin system in the ^{31}P NMR spectrum corresponding to the 93%

component of the crude reaction mixture. Yield: 333 mg, 67%. Elemental analysis (calc./expt.): C – 43.46/43.10, H – 7.50/7.23, N – 2.82/3.09. ^{1}H NMR (CDCl$_3$, 400.19 MHz, 298.15 K): δ_H 1.23 (d, J = 6.1 Hz, 3H), 1.34 (d, J = 15.2 Hz, 9H), 1.34 (d, J = 6.2 Hz, 3H), 1.41 (d, J = 18.9 Hz, 9H), 1.44 (dt, J = 16.4, 1.0 Hz, 9H), 2.32 (dd, J = 12.4, 1.1 Hz, 3H), 3.74 (septet of dd, J = 6.1, 2.9, 1.2 Hz, 1H). ^{31}P{^{1}H} NMR (CD$_2$Cl$_2$, 162.00 MHz, 298.15 K): δ_P -47.7 (dd, J = 260, 166 Hz, 1P), 52.7 (dd, J = 260, 33 Hz, 1P), 82.3 (dd, J = 260, 33 Hz, 1P). ^{19}F NMR (CD$_2$Cl$_2$, 376.55 MHz, 298.15 K): δ_F -78.74 (s).

[**9$^\mathbf{i}$Pr**][OTf]: Neat ^{i}PrNC (210 mg, 3 mmol) was added at once to a stirred solution of [**4Me**][OTf] (516 mg, 1 mmol) in 4 mL CH$_2$Cl$_2$ at 25 °C to immediately give a reddish brown solution. This crude reaction mixture was stirred for 24 h at which point a ^{31}P NMR assay showed complete conversion of resonances due to the starting materials to a new AGMX spin system. All volatiles were removed under vacuum to yield a brown powder. This powder was redissolved in a minimum amount of MeCN, layered with Et$_2$O, and kept at -30 °C for 7 days to yield yellow-orange crystals suitable for X-ray crystallography. Three crops of crystals were obtained over 7 days, combined after decanting the supernatant from each, and dried under vacuum to yield [**9$^\mathbf{i}$Pr**][OTf] as a yellow-orange powder. Yield: 305 mg, 52%. Elemental analysis (calc./expt.): C – 45.13/44.89, H – 7.92/7.83, N – 2.39/2.57. ^{1}H NMR (CD$_2$Cl$_2$, 300.53 MHz, 298.15 K): δ_H 1.20 (d, J = 4.1 Hz, 3H, C^3), 1.24 (d, J = 17.0 Hz, 9H, C$^{10/11/12}$), 1.33 (d, J = 14.6 Hz, 9H, C$^{10/11/12}$), 1.33 (m, 3H, C^2), 1.44 (d, J = 17.6 Hz, 9 H, C^9), 1.48 (d, J = 14.6 Hz, 9H, C$^{10/11/12}$), 2.29 (d, J = 11.6 Hz, 3H, C^4), 4.28 (m, J = 5.9 Hz, 2.2 Hz, 1H, C^1). ^{13}C{^{1}H} NMR (CD$_2$Cl$_2$, 100.63 MHz, 298.15 K): δ_C 176.08 (m, J = 87, 36 Hz, C^{13}), 121.5 (q, $^1J_{CF}$ = 321 Hz, SO$_3$CF$_3$), 65.9 (dd, $^3J_{CP}$ = 26.5, 19.8 Hz, C^1), 38.5 (ddd, $^1J_{CP}$ = 32 Hz, $^2J_{CP}$ = 15 Hz, $^3J_{CP}$ = 3 Hz, C^5), 37.4 – 36.6 (m, C$^{6/7/8}$), 32.8 – 32.2 (m, C$^{6/7/8}$), 31.9 (dt, $^2J_{CP}$ = 15Hz, $^3J_{CP}$ = 5 Hz, C$^{10/11/12}$), 31.6 (ddd, $^2J_{CP}$ = 14 Hz, $^3J_{CP}$ = 7, 1 Hz, C$^{10/11/12}$), 29.8 (ddd, $^2J_{CP}$ = 14.0 Hz, $^3J_{CP}$ = 8, 6 Hz, C$^{10/11/12}$), 26.1 (d, $^2J_{CP}$ = 4 Hz, C^9), 23.6 (d, $^4J_{CP}$ = 2 Hz, C^3), 23.0 (d, $^4J_{CP}$ = 2 Hz, C^2), 8.0 (d, $^1J_{CP}$ = 21 Hz, C^4) ^{31}P{^{1}H} NMR (CD$_2$Cl$_2$, 121.66 MHz, 298.15 K): δ_P -58.1 (ddd, J = 429, 294, 6 Hz, P^2), -13.0 (ddd, J = 294, 333, 16, P^3), 14.9 (ddd, J = 333, 48, 6, P^4), 72.1 (ddd, J = 429, 48, 16 Hz, P^2). ^{19}F NMR (CD$_2$Cl$_2$, 282.78 MHz, 298.15 K): δ_F -78.60 (s). ESI-MS: 436.2563 m/z [**9$^\mathbf{i}$Pr**]$^+$ (calculated: 436.2575 m/z).
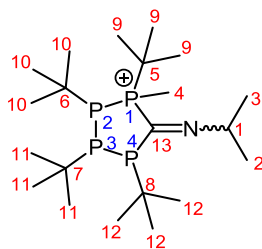
[9Pent][OTf]: Prepared employing the same procedure and scale as [**9ⁱPr**][OTf] but 1-pentyl-isocyanide (PentNC) was employed instead of ⁱPrNC. The product was characterized in-situ without isolation. ^{1}H NMR (CD$_2$Cl$_2$, 499.89 MHz, 298.15 K): δ_H 0.89 (t, J = 7.0 Hz, 3H), 1.23 (d, J = 14.9 Hz, 9H), 1.32 (d, J = 14.9 Hz, 9H), 1.42 (d, J = 17.6 Hz, 9H), 1.48 (d, J = 16.8 Hz, 9H), 2.33 (dd, J = 11.6, 0.8 Hz, 3H), 4.02-4.22 (m, 2H). ^{13}C{^{1}H} NMR (CD$_2$Cl$_2$, 125.71 MHz, 298.15 K): δ_C 15.6 (s), 24.1 (s), 27.4 (d, J = 4 Hz), 31.1-31.4 (m), 31.5 (s), 32.2 (s), 33.1-33.4 (m), 33.6-34.0 (m), 38.22 (ddd, J = 29, 17, 5 Hz), 39.71 (ddd, J = 32, 15, 3 Hz), 40.44 (dd, J = 23, 14 Hz), 67.8 (dd, J = 27, 21 Hz), 122.8 (q, J = 321 Hz), 180.7 (ddt, J = 85, 38, 6 Hz). ^{31}P{^{1}H} NMR (CD$_2$Cl$_2$, 121.66 MHz, 298.15 K): δ_P -57.8 (ddd, J = 428, 293, 6 Hz, 1P), -13.1 (ddd, J = 332, 293, 17 Hz, 1P), 15.9 (ddd, J = 332, 45, 5 Hz, 1P), 71.8 (ddd, J = 426, 45, 17 Hz, 1P). ^{19}F NMR (CD$_2$Cl$_2$, 282.78 MHz, 298.15 K): δ_F -78.60 (s).

[12Cl][OTf]: With exclusion of light, ^{t}BuPCl$_2$ (160 mg, 1 mmol), AgOTf (257 mg, 1 mmol), and *dmap* (122 mg, 1 mmol) were combined in 4 mL MeCN and stirred for 24 h. The resulting white suspension was filtered to remove AgCl and the filtrate was analysed by ^{31}P NMR spectroscopy and found to exhibit a single peak that matched the resonance assigned to [**12Cl**][OTf] in the reaction of [**4Cl**][OTf] and *dmap* (see below) The filtrate was concentrated to 1 mL, layered with Et$_2$O, and kept at -30 °C for 2 days to yield colourless crystals identified as [**12Cl**][OTf] by X-Ray crystallography. Yield: 327 mg, 83 %. Elemental analysis (calc./expt.): C – 31.56/31.44, H – 3.31/3.54, N – 9.20/8.89. ^{1}H NMR (CD$_3$CN, 300.53 MHz, 298.15 K): δ_H 1.09 (d, J = 16.1 Hz, 9H), 3.22 (s, 6H), 6.72-7.27 (m, 2H), 7.79-8.28 (m, 2H). ^{13}C{^{1}H} NMR (CD$_2$Cl$_2$, 100.63 MHz, 298.15 K): 23.8 (d, $^2J_{CP}$ = 20 Hz, C(*CH$_3$*)$_3$), 39.0 (d, $^1J_{CP}$ = 38 Hz, *C*(CH$_3$)$_3$), 40.5 (s, N(*CH$_3$*)$_2$), 109.1 (d, J_{CP} = 5 Hz, *dmap*), 121.3 (q, $^1J_{CF}$ = 323 Hz, OTf), 142.4 (d, J_{CP} = 20 Hz, *dmap*), 158.3 (s, *dmap*). ^{31}P NMR (CD$_3$CN, 121.66 MHz, 298.15 K): δ_P 158.6 (s). ^{19}F NMR (CD$_2$Cl$_2$, 282.78 MHz, 298.15 K): δ_F -78.88 (s). ESI-MS: 245.10 *m/z*, [**12Cl**]$^+$.

13: This compound was formed by thermal decomposition of [**7**][OTf] in 1,2-difluorobenzene in the presence of 20 equivalents of 1,3-cyclohexadiene and characterized in-situ without isolation. ^{1}H NMR (C$_6$D$_6$, 499.89 MHz, 298.15 K): δ_H 1.09 (d, [3]J_{PH} = 12 Hz, C^9, 9H), 1.29 (d, [3]J_{PH} = 12 Hz, C^{10}, 9H) 1.65 (br s, C^5, 2H), 1.86 (br s, C^6, 1H), 2.82 (br s, C^1, 1H), 2.98 (br s, C^4, 1H), 6.01 (br m, C^2 + C^3, 2H). See Figure S13 (Supporting Information). ^{13}C{^{1}H} NMR (C$_6$D$_6$, 100.63 MHz, 298.15 K): δ_C 23.9 (d, [2]J_{CP} = 3 Hz, C^6) 25.9 (dd, [2]J_{CP} = 23 Hz, [3]J_{CP} = 5 Hz, C^5), 27.6 (dd, [1]J_{CP} = 29 Hz, [2]J_{CP} = 4Hz, C^1), 29.8 (dd, [1]J_{CP} = 32 Hz, [2]J_{CP} = 1 Hz, C^4), 28.9-29.4 (m, C^7, C^8), 30.1 (dd, [2]J_{CP} = 15 Hz, [3]J_{CP} = 5 Hz, C^9), 31.0 (dd, [2]J_{CP} = 15 Hz, [3]J_{CP} = 7 Hz, C^{10}), 129.9 (d, [2]J_{CP} = 6 Hz, C^3), 134.5 (dd, [2]J_{CP} = 11, [3]J_{CP} = 5 Hz, C^2). ^{31}P NMR (C$_6$D$_6$, 162.00 MHz, 298.15 K): δ_P -12.9 (d, [1]J_{PP} = 263 Hz, P^A), 4.8 (d, [1]J_{PP} = 263 Hz, P^B). ESI-MS: 273.15 [**13**+O+H]$^+$.
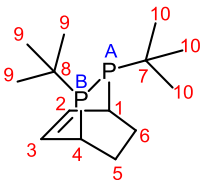
[(*dmap*)$_2$P^{t}Bu][OTf]$_2$: With exclusion of light, ^{t}BuPCl$_2$ (160 mg, 1 mmol), AgOTf (514 mg, 2 mmol), and *dmap* (244 mg, 1 mmol) were combined in 5 mL MeCN and stirred for 2 h. The resulting white suspension was filtered to remove AgCl. Analysis of the filtrate by ^{31}P NMR spectroscopy showed a single peak that matched the resonance assigned to [(*dmap*)$_2$P^{t}Bu][OTf] in the reaction of [**4F**][OTf] and *dmap* (see below). The compound was found to be thermally labile and decomposed to a brown oil under vacuum precluding isolation. Spectroscopic data for a sample stored at -30 °C are as follows: ^{1}H NMR (CD$_2$Cl$_2$, 300.53 MHz, 298.15 K): δ_H 1.33 (d, [3]J_{PH} = 17.3 Hz, 9H), 3.23 (s, 12H), 7.00 (d, J = 7.8 Hz, 4H), 8.24 (d, J = 7.7 Hz, 4H). ^{13}C{^{1}H} NMR (CD$_2$Cl$_2$, 75.57 MHz, 298.15 K): δ_C 25.8 (d, J = 20.3 Hz), 37.5 (d, J = 31.1 Hz), 40.65 (s), 109.5 (s), 121.1 (q, [1]J_{CF} = 321.1 Hz), 143.9 (s), 157.5 (s). ^{31}P{^{1}H} NMR (CD$_2$Cl$_2$, 121.66 MHz, 298.15 K): δ_P 140.0 (s). ^{19}F NMR (CD$_2$Cl$_2$, 282.78 MHz, 298.15 K): δ_F -78.50 (s).

Thermal decomposition of [7]$^+$: Solid [**7**][OTf] (110 mg, 0.2 mmol), neat 1,3-cyclohexadiene (160 mg, 2 mmol), and 1,2-difluorobenzene (0.4 mL) were combined in a J-Young NMR tube and placed in an 80 °C oil bath for 2 h and then assayed by ^{31}P NMR spectroscopy. Complete conversion of [**7**]$^+$ to [**12Me**]$^+$, **13**, and minor amounts of **2** were detected. Volatiles were removed and the residue extracted with benzene and assayed by ^{31}P and ^{1}H NMR. Analysis of

the benzene extract by ESI-MS showed the [13+O+H]$^+$ peak at 273.15 m/z due to oxidation during data acquisition under ambient atmosphere. Attempts to separate **13** from the small amounts of **2** and impurities formed during the reaction were unsuccessful. The ^{31}P and ^{1}H NMR spectra of the reaction mixtures and benzene extract are given below. A parallel experiment was conducted where [**7**][OTf] was heated in the absence of 1,3-cyclohexadiene and showed conversion to [**12Me**][OTf] and **2** with no evidence of **13** (see Figure S12, Supporting Information).

[12Me][OTf]: This compound was characterized in-situ following the above-mentioned thermal decomposition of [**7**][OTf] in the absence of 1,3-cyclohexadiene in 1,2-difluorobenzene. The reaction mixture was dried under vacuum and redissolved in CD$_2$Cl$_2$ for analysis. ^{1}H NMR (CD$_2$Cl$_2$, 300.53 MHz, 298.15 K): δ_H 1.01 (d, $^3J_{PH}$ = 13.8 Hz, 9H), 1.68 (d, $^2J_{PH}$ = 7.2 Hz, 3H), 3.23 (s, 6 H). ^{13}C{^{1}H} NMR (CD$_2$Cl$_2$, 100.63 MHz, 298.15 K): δ_C 24.9 (d, $^2J_{CP}$ = 16 Hz, C(CH$_3$)$_3$), 32.6 (d, $^1J_{CP}$ = 21 Hz, P-CH$_3$), 40.0 (br s, C(CH$_3$)$_3$), 40.3 (br, s, N(CH$_3$)$_2$), 108.4 (br s, *dmap*), 120.9 (q, $^1J_{CF}$ = 321 Hz, OTf), 144.3 (br d, J_{CP} = 16 Hz, *dmap*), 157.4 (s, *dmap*). ^{19}F NMR (CD$_2$Cl$_2$, 282.78 MHz, 298.15 K): δ_F -78.91 (s). ESI-MS: 225.15 *m/z*, [**12Me**]$^+$.

X-ray crystallography: X-ray diffraction experiments on [**5Me**][OTf], [**5Ph**][OTf]•Et$_2$O, [**8^{i}Pr**][OTf] and [**12Cl**][OTf] were carried out at 100(2) K on a Bruker APEX II CCD diffractometer using Mo-K$_\alpha$ radiation (λ = 0.71073 Å), while [**9^{i}Pr**][OTf] was carried out at 100(2) K Bruker Microstar CCD rotating anode diffractometer using Cu-K$_\alpha$ (λ = 1.54178 Å). Intensities were integrated[78] and absorption corrections were based on equivalent reflections using SADABS.[79] Structures [**5Me**][OTf], [**5Ph**][OTf]•Et$_2$O, [**8^{i}Pr**][OTf] and [**12Cl**][OTf] were solved using Superflip,[80] while [**9^{i}Pr**][OTf] was solved in ShelXT using intrinsic methods[81] all of the structures were refined against F^2 in SHELXL[81,82] using Olex2.[83] All of the non-hydrogen atoms were refined anisotropically. All of the hydrogen atoms were located geometrically and refined using a riding model. In the case of [**5Ph**][OTf]•Et$_2$O, [**9^{i}Pr**][OTf] and [**12Cl**][OTf] there was disorder in one of the triflate anions. The occupancies of the fragments was determined by refining them against a free variable with the sum of the two sites set to equal 1. The occupancies were then fixed at the refined values, and restraints and constraints were used to maintain sensible geometries and thermal parameters. In the case of [**5Ph**][OTf]•Et$_2$O the diethyl

ether was disordered over two positions across the *c* glide the occupancies of these two positions was 50%. Crystallographic data for compounds [**5Me**][OTf], [**5Ph**][OTf]•Et$_2$O, [**8^{i}Pr**][OTf], [**9^{i}Pr**][OTf] and [**12Cl**][OTf] have been deposited with the Cambridge Crystallographic Data Centre as supplementary publication CCDC 1510725-1510729. Copies of the data can be obtained free of charge on application to CCDC, 12 Union Road, Cambridge CB2 1EZ, UK [fax(+44) 1223 336033, e-mail: deposit@ccdc.cam.ac.uk]. Crystal structure and refinement data are given in Table S5 (see Supporting Information).

Computational details: All calculations were performed using the Gaussian 09 suite.[84] A benchmarking study was performed using experimental bond lengths in three-membered phosphorus rings **1** and [**3Me**]$^+$ (see Supporting Information). The functionals investigated were selected based on previous use in related systems.[27] The geometries of both **1** and [**3Me**]$^+$ were optimized in the gas phase (298 K) with various basis set/functional combinations. GD3 dispersion was employed in all cases with the exception of MP2 calculations. The starting geometry used in all benchmarking optimizations was that previously obtained experimentally by single crystal X-ray diffraction. Values of d(P–P) show a small degree of functional dependence, with PBE1PBE yielding the closest match to experimental bond lengths. Despite the basis set 6- 311G(d,p) yielding the most accurate results with respect to d(P–P), the basis set 6-311+G(d,p) was selected for this computational study in order to enable future continuation to anionic species, where basis sets with diffuse functions are essential.

Volume-based thermodynamics: Lattice enthalpies were estimated from the relationship between lattice volumes and energies as generalized by Jenkins, Passmore and Glasser[52,53] as per the following equation:

$$H_{lat.} = 2I\left(\frac{\alpha}{\sqrt[3]{V_m}} + \beta\right) + p\text{RT}$$

I is the ionicity, which is unitary for singly-charged salts of the type [A][X]. The molar volume, V_m (in nm^3) was obtained experimentally from X-ray crystallography by dividing the unit cell volume by the number of formula units within the cell. The quantities α and β are empirical parameters determined to be 117.3 kJ mol^{-1} nm and 51.9 kJ mol^{-1}, respectively, from least-squares analysis of experimentally known lattice enthalpies for singly charged salts and their

ionic volumes. The first expression in the above equation represents the lattice potential at 0 K, $U_{lat.}$. Conversion of $U_{lat.}$ to $H_{lat.}$ is accomplished by a thermal correction, pRT, which includes a consideration of the ionic shapes *via* the prefactor p to account for number of accessible vibrational modes. For salts containing non-linear polyatomic ions, as in the case of all species considered here, p equals 2, R is the gas constant (8.314×10^{-3} kJ mol^{-1} K^{-1}), and T is the standard temperature 298.15 K. The lattice enthalpies of [**3Me**][OTf] and [**5Me**][OTf] are 397 kJ mol^{-1} and 380 kJ mol^{-1}, respectively, with errors estimated to be 4% for salts having $H_{lat.} < 5000$ kJ mol^{-1}.

Jenkins and Glasser have also demonstrated[54] the good proportionality ($r^2 = 0.90$, $n = 65$) of lattice entropies and the molar volume, V_m (in nm^3), for ionic solids as per the following equation:

$$S_{lat.} = kV_m + c$$

Here, k and c are empirical parameters determined from least-squares analysis of known lattice entropies and volumes to be 1360 J K^{-1} mol^{-1} and 15 J K^{-1} mol^{-1}, respectively. The resulting $S_{lat.}$ values for [**3Me**][OTf] and [**5Me**][OTf] are 752 J mol^{-1} K^{-1} and 798 J mol^{-1} K^{-1}, respectively, with an estimated error of 11 %.

Supporting Information.

The following files are available free of charge.

Supporting figures, tables of ^{31}P NMR chemical shifts, Cartesian coordinates for calculated structures (PDF)

Crystallographic data (CIF)

Corresponding Author

Ian Manners: ian.manners@bristol.ac.uk

Author Contributions

The manuscript was written through contributions of all authors. All authors have given approval to the final version of the manuscript.

References

[1] Meijere, A. Bonding properties of cyclopropane and their chemical consequences. *Angew. Chem. Int. Ed.*, **1979**, *18*, 809-886; Liebman, J. F.; Greenberg, A. Survey of the heats of formation of three-membered-ring species. *Chem. Rev.*, **1989**, *89*, 1225-1246; Dewar, M. J. S. Chemical Implications of σ conjugation. *J. Am. Chem. Soc.*, **1984**, *106*, 669-682; Cremer, D. Pros and cons of σ-aromaticity. *Tetrahedron*, **1988**, *44*, 7427-7454.

[2] Nuyken, O.; Pask, S. D. Ring-Opening Polymerization—An Introductory Review. *Polymer*, 2013, *5*, 361-403.

[3] Reissig, H; Zimmer, R. Thrilling Strain! Donor – Acceptor-Substituted Cyclobutanes for the Synthesis of (Hetero)Cyclic Compounds. *Chem. Rev.*, **2003**, *103*, 1151-1196; Schneider, T. F.; Kaschel, J.; Werz, D. B. A New Golden Age for Donor – Acceptor Cyclopropanes. *Angew. Chem. Int. Ed.*, **2014**, *53*, 5504-5523.

[4] Chattaraj, P. K.; Cedillo, A.; Parr, R. G. Appraisal of Chemical Bond Making, Bond Breaking, and Electron Transfer in Solution in the Light of the Principle of Maximum Hardness. *J. Org. Chem.*, **1995**, *60*, 4707-4714.

[5] Yu, M.; Pagenkopf, B. L. Formal [3 + 2] Cycloadditions of Donor - Acceptor Cyclopropanes and Nitriles. *J. Am. Chem. Soc.*, **2003**, *125*, 8122-8123.

[6] Cui, B.; Ren, J.; Wang, Z. TfOH-Catalyzed Formal [3 + 2] Cycloaddition of Cyclopropane 1,1- Diesters with Nitriles. *J. Org. Chem.*, **2014**, *79*, 790-796.

[7] Yu, M.; Pagenkopf, B. L. A Powerful New Strategy for Diversity-Oriented Synthesis of Pyrroles from Donor − Acceptor Cyclopropanes and Nitriles. *Org. Lett.*, **2003**, *5*, 5099-5101.

[8] Moustafa, M. A. R. M.; Pagenkopf, B. L. Synthesis of 5-Azaindoles via a Cycloaddition Reaction between Nitriles and Donor - Acceptor Cyclopropanes. *Org. Lett.*, **2010**, *12*, 3168-3171.

[9] Chakrabarty, S.; Chatterjee, I.; Wibbeling, B., Daniliuc, C. G.; Studer, A. Stereospecific Formal [3 + 2] Dipolar Cycloaddition of Cyclopropanes with Nitrosoarenes : An Approach to Isoxazolidines . *Angew. Chem. Int. Ed.*, **2014**, *53*, 5964-5968.

[10] Vemula, N.; Stevens, A. C.; Schon, T. B.; Pagenkopf, B. L. The [4+2] cycloaddition of donor–acceptor cyclobutanes and nitrosoarenes. *Chem. Commun.*, **2014**, *50*, 1668-1670.

[11] Shenje, R.; Martin, M. C.; France, S. A catalytic diastereoselective formal [5+2] cycloaddition approach to azepino[1,2-a]indoles: Putative donor-acceptor cyclobutanes as reactive intermediates. *Angew. Chem. Int. Ed.*, **2014**, *53*, 13907-13911.

[12] Parsons, A. T., Johnson, J. S. Formal [4 + 2] Cycloaddition of Donor - Acceptor Cyclobutanes and Aldehydes : Stereoselective Access to Substituted Tetrahydropyrans. *J. Am. Chem. Soc.*, **2009**, *131*, 14202-14203.

[13] Grover, H. K.; Emmett, M. R.; Kerr, M. A. Carbocycles from donor-acceptor cyclopropanes. *Org. Biomol. Chem.*, **2015**, *13*, 655-671.

[14] Finnegan, W. G.; Henry, R. A. An improved synthesis of 5-substituted tetrazoles. Lofquist, R. *J. Am. Chem. Soc.*, **1958**, *80*, 3908-3911.

[15] Liang, M.; Manners, I. Poly(thionylphosphazenes): A New Class of Inorganic Polymers with Skeletal Phosphorus, Nitrogen, and Sulfur(VI) Atoms. *J. Am. Chem. Soc.*, **1991**, *113*, 4044-4045.

[16] Musgrave, R. A.; Russell, A. D. Strained ferrocenophanes. Manners, I. *Organometallics*, **2013**, *32*, 5654-5667.

[17] Priegert, A. M.; Rawe, B. W.; Serin, S. C.; Gates, D. P. Polymers and the p-block elements. *Chem. Soc. Rev.*, **2016**, *45*, 922-953.

[18] Herbert, D. E.; Mayer, U. F. J.; Manners, I. Strained metallocenophanes and related organometallic rings containing π-hydrocarbon ligands and transition-metal centers. *Angew. Chem. Int. Ed.*, **2007**, *46*, 5060-5081.

[19] Vanderark, L. A.; Clark, T. J.; Rivard, E.; Manners, I.; Slootweg, J. C.; Lammertsma, K. Anionic ring-opening polymerization of a strained phosphirene: a route to polyvinylenephosphines. *Chem. Commun.*, **2006**, 3332-3333.

[20] Zhang, Y.; Huynh, K.; Manners, I.; Reed, C. Ambient temperature ring-opening polymerisation (ROP) of cyclic chlorophosphazene trimer $[N_3P_3Cl_6]$ catalyzed by silylium ions. *Chem. Commun.*, **2008**, 494-496.

[21] He, G.; Shynkaruk, O.; Lui, M. W.; Rivard, E. Small Inorganic Rings in the 21st Century: From Fleeting Intermediates to Novel Isolable Entities. *Chem. Rev.*, **2014**, *114*, 7815-7880.

[22] Baudler, M.; Glinka, K. Monocyclic and Polycyclic Phosphanes. *Chem. Rev.*, **1993**, *93*, 1623-1667.

[23] Baudler, M.; Hahn, J.; Clef, E. Triethyl-cyclotriphosphan, Trimethyl-cyclotriphosphan; Gleichgwichte zwischen Cyclophosphanen (PR)$_n$ bei erhöhten Temperaturen. *Z. Naturforsch*, **1984**, *39B*, 438-444.

[24] Baudler, M.; Hahn, J.; Dietsch, H.; Fürstenberg, G. Contributions to the Chemistry of Phosphorus: Tri-butyl-cyclotriphosphane. *Z. Naturforsch.*, **1976**, *31B*, 1305-1310.

[25] Dyker, C. A.; Burford, N.; Menard, G.; Lumsden, M. D.; Decken, A. Monocyclic di- and triphosphinophosphonium cations: New foundational frameworks for catena-phosphorus chemistry. *Inorg. Chem.*, **2007**, *46*, 4277-4285.

[26] Chitnis, S. S.; Whalen, M.; Burford, N. Influence of charge and coordination number on bond dissociation energies, distances, and vibrational frequencies for the phosphorus-phosphorus bond. *J. Am. Chem. Soc.*, **2014**, *136*, 12498-12506.

[27] a) Burford, N.; Cameron, T. S.; Ragogna, P. J.; Ocando-Mavarez, E.; Gee, M.; McDonald, R.; Wasylishen, R. E. Phosphine ligand exchange at a phosphine Lewis acceptor: The first structural characterization of homoleptic phosphinophosphonium salts. *J. Am. Chem. Soc.*, **2001**, *123*, 7947-7948. b) Robertson, A. P. M.; Dyker, C. A.; Gray, P. A.; Patrick, B. O.; Decken, A.; Burford, N. Diverse Reactivity of the cyclo-Diphosphinophosphonium Cation [(P^{t}Bu)$_3$Me]$^+$: Parallels with Epoxides and New catena -Phosphorus Frameworks. *J. Am. Chem. Soc.*, **2014**, *136*, 14941-14950. c) Bamford, K. L.; Chitnis, S. S.; Stoddard, R. L.; McIndoe, J. S.; Burford, N. Bond fission in monocationic frameworks: diverse phosphinophosphonium cations. *Chem. Sci.*, **2016**, *7*, 2544-2552.

[28] Gudat, D. Diazaphospholenes: N -Heterocyclic Phosphines between Molecules and Lewis Pairs. *Acc. Chem. Res.*, **2010**, *43*, 1307-1316. Burck, S.; Gudat, D.; Nieger, M. Metal-assisted, reversible phosphinyl phosphination of the carbon-nitrogen triple bond in a nitrile. *Angew. Chem. Int. Ed.*, **2004**, *43*, 4801-4804. Hajdok, I.; Lissner, F.; Nieger, M.; Strobel, S.; Gudat, D. Cleavage of Polarized P-P Bonds in N-Heterocyclic Diphosphines in Reactions with Metal Olefin Complexes. *Organometallics*, **2009**, *28*, 1644-1651. Burck, S.; Götz, K.; Kaupp, M.; Nieger, M.; Weber, J.; auf der Günne, J. S.; Gudat, D. Diphosphines with Strongly Polarized P-P Bonds: Hybrids between Covalent Molecules and Donor-Acceptor Adducts with Flexible Molecular Structures. *J. Am. Chem. Soc.*, **2009**, *131*, 10763-10774.

[29] Baudler, M.; Glinka, K; Cowley, A. H.; Pakulski, M. Organocyclophosphanes. *Inorg. Synth.*, **1989**, *25*, 1-5.

[30] Weigand, J. J.; Burford, N., Davidson, R. J.; Cameron, T. S.; Seelheim, P. New Synthetic Procedures to Catena-Phosphorus Cations: Preparation and Dissociation of the First cyclo-Phosphino-halophosphonium Salts. *J. Am. Chem. Soc.*, **2009**, *131*, 17943-17953.

[31] Holthausen, M. H., Knackstedt, D., Burford, N.; Weigand, J. J. Phosphenium-Insertion and Chloronium-Addition Reactions Involving the cyclo-Phosphanes (^{t}BuP)$_n$ (n=3, 4). *Aust. J. Chem.*, **2013**, *66*, 1155-1162.

[32] Caputo, C. P.; Hounjet, L. J.; Dobrovetsky, R.; Stephan, D. W. Lewis acidity of organofluorophosphonium salts: hydrodefluorination by a saturated acceptor. *Science*, **2013**, *135*, 18308-18310.

[33] Stein, T. V.; Perez, M.; Dobrovetsky, R.; Winkelhaus, D.; Caputo, C.B.; Stephan, D. W. Electrophilic Fluorophosphonium Cations in Frustrated Lewis Pair Hydrogen Activation and Catalytic Hydrogenation of Olefins. *Angew. Chem. Int. Ed.*, **2015**, *54*, 10178-10182.

[34] a) Ferao, A. E.; Streubel, R. Thiaphosphiranes and Their Complexes: Systematic Study on Ring Strain and Ring Cleavage Reactions. *Inorg. Chem.*, **2016**, *55*, 9611-9619. b) Helten, H.; Pérez, J. M.; Daniels, J.; Streubel, R. First brønsted acid-induced ring expansion of an oxaphosphirane complex: a combined experimental and DFT study. *Organometallics* **2009**, *28*, 1221-1226. c) Espinosa, A.; de las Heras, E.; Streubel, R. Oxaphosphirane-borane complexes: Ring strain and migratory insertion/ring-opening reactions. *Inorg. Chem.*, **2014**, *53*, 6132-6140.

[35] Schiffer, H.; Ahlrichs, R.; Haser, M. Theoretical investigation of next neighbour interactions and ring strain in linear and monocyclic phosphanes. *Theor. Chim. Acta.*, **1989**, *75*, 1-10.

[36] Glukhovtsev, M. N.; Bach, R. D.; Laiter, S. High-Level Computational Study on the Thermochemistry of Saturated and Unsaturated Three- and Four-Membered Nitrogen and Phosphorus Rings. *Int. J. Quant. Chem.*, **1997**, *62*, 373-384.

[37] Inagaki, S.; Yoshikawa, K.; Hayano, Y. σ- -Electrons in silanes and phosphines: geminal bond interaction, angle strain, and delocalizability. *J. Am. Chem. Soc.*, **1993**, *115*, 3706-3709.

[38] Inagaki, S.; Ishitani, Y.; Kakefu, T. Geminal Delocalization of σ-Electrons and Ring Strains. *J. Am. Chem. Soc.*, **1994**, *116*, 5954-5958.

[39] Nguyen, M. T.; Dransfeld, A.; Landuyt, L.; Vanquickenborne, L. G.; Schleyer, P. v. R. Calculated properties and ring-chain rearrangements of Triphosphirane (P_3H_3). *Eur. J. Inorg. Chem.*, **2000**, 103-112.

[40] Schoeller, W. W.; Staemmler, V.; Rademacher, P.; Niecke, E. heoretical studies on inorganic ring systems. Tetraphosphabicyclobutane, cyclotriphosphane, and white phosphorus: ring strain and hybridization. *Inorg. Chem.*, **1986**, *25*, 4382-4385.

[41] Wheeler, S. E.; Houk, K. N.; Schleyer, P. v. R.; Allen, W. D. A Hierarchy of homodesmotic reactions for thermochemistry. *J. Am. Chem. Soc.*, **2009**, *131*, 2547-2560.

[42] See references in: Prasang, C.; Scheschkewitz, D. Reactivity in the periphery of functionalised multiple bonds of heavier group 14 elements. *Chem. Soc. Rev.*, **2016**, *45*, 900-921; Power, P. P. Interaction of multiple bonded and unsaturated heavier main group compounds with hydrogen, ammonia, olefins, and related molecules. *Acc. Chem. Res.*, **2011**, *44*, 627-637.

[43] Cameron, T. S.; Deckan, A.; Grein, F.; Knapp, C.; Passmore, J.; Rautiainen, J. M.; Shuvaev, K. V.; Thombson, R. C.; Wood, D. J. Preparation and Characterization of $(CNSSS)_2(A)_2$ ($A = AsF_6^-$, SbF_6^-, $Sb_2F_{11}^-$) Containing the O_2-like 5,5′-Bis(1,2,3,4-trithiazolium) Dication: The Second Example of a Simple Nonsterically Hindered Main-Group Diradical That Retains Its Paramagnetism in the Solid State. *Inorg. Chem.*, **2010**, *49*, 7861-7879.

[44] Decken, A.; Ebdah, M.; Kowalczyk, R. M.; Landee, C. P.; McInnes, E. J. L.; Passmore, J.; Shuvaev, K. V.; Thompson, L. K. Tuning Intermolecular Magnetic Exchange Interactions in the Solids $C_xF_{2x}(CNSSS)_2(AsF_6)_2$: Structural, EPR, and Magnetic Characterization of Dimeric (x = 2, 4) Diradicals. *Inorg. Chem.*, **2007**, *46*, 7756-7766.

[45] Decken, A.; Mattar, S. M., Passmore, J., Shuvaev, K. V.; Thompson, L. K. Toward a More General Synthetic Route to Paramagnetic Solids Containing RCNSSS•+ Radical Cations. A Structure−Property Correlation for RCNSSS•+ ($R = F_5C_2$, Cl_3C). *Inorg. Chem.*, **2006**, *45*, 3878-3886.

[46] Boyle, P. D.; Parsons, S.; Passmore, J.; Wood, D. J. The preparation and characterization of the paramagnetic solid bis(1,2,3,4-trithiazolium)bis(hexafluoroarsenate) containing the dioxygen-like dication diradical $SSSNCCNSSS^{2+}$. *J. Chem. Soc. Chem. Commun.*, **1993**, 199-201.

[47] Cameron, T. S.; Haddon, R. C.; Mattar, S. M.; Parsons, S.; Passmore, J.; Ramirez, A. P. Synthesis, characterization, and x-ray crystal structure of the paramagnetic solid 5-(trifluoromethyl)-1,2,3,4-trithiazolium hexafluoroarsenate, containing the novel, planar 7π CF_3CNSSS^+ radical cation. *Inorg. Chem.*, **1992**, *31*, 2274-2279.

[48] Pelties, S.; Ehlers, A. W.; Wolf, R. Insertion of phenyl isothiocyanate into a P − P bond of a nickel-substituted bicyclo[1.1.0]tetraphosphabutane. *Chem. Commun.*, **2016**, *52*, 6601-6604.

[49] Hoffman, N.; Wismach, C.; Jones, P. G.; Streubel, R.; Huy, N. H. T.; Mathey, F. Synthesis of the first 1, 2, 3, 4-azatriphospholene complex. *Chem. Commun.*, **2002**, 454-455.

[50] Burck, S.; Gudat, D.; Nieger, M. Metal-Assisted, Reversible Phosphinyl Phosphination of the Carbon–Nitrogen Triple Bond in a Nitrile. *Angew. Chem. Int. Ed.*, **2007**, *46*, 2919-2922.

[51] Antosik, M.; Galka, M.; Malanowski, S. K. Vapor−Liquid Equilibrium for Acetonitrile + Propanenitrile and 1-Pentanamine + 1-Methoxy-2-propanol. *J. Chem. Eng. Data*, **2004**, *49*, 11-17.

[52] Jenkins, H. D. B.; Tudela, D.; Glasser, L. Lattice potential energy estimation for complex ionic salts from density measurements. *Inorg. Chem.*, **2002**, *41*, 2364-2367.

[53] Jenkins, H. D. B.; Roobottom, H. K.; Passmore, J.; Glasser, L. Relationships among ionic lattice energies, molecular (formula unit) volumes, and thermochemical radii. *Inorg. Chem.*, **1999**, *38*, 3609-3620.

[54] Jenkins, H. D. B.; Glasser, L. Standard Absolute Entropy, S_{298o}, Values from Volume or Density. 1. Inorganic Materials. *Inorg. Chem.*, **2003**, *42*, 8702-8708.

[55] Putnam, W. E.; McEachern, D. M.; Kilpatrick, J. E. Entropy and Related Thermodynamic Properties of Acetonitrile (Methyl Cyanide). *J. Chem. Phys.*, **1965**, *42*, 749-755.

[56] Energy values calculated in the solvent phase using PCM calculations exhibited the same trend (see Table S9 in Supporting Information). Gas-phase values are given here to facilitate comparison between reactions with nitriles and isonitriles, which were conducted in different solvents.

[57] Moderhack, D. Four-membered rings from isocyanides: Developments since the mid-1980s. *ARKIVOC*, **2014**, *2*, 406-451.

[58] Weidenbruch, M.; Hamann, J.; Peters, K.; Schnering, H. G. v.; Marsmann, H. Siliciumverbindungen mit starken intramolekularen sterischen wechselwirkungen: XLVIII. Trisilacyclobutanimine: Moleküstrukturen und lichtinduzierte reaktionen. *J. Organomet. Chem.*, **1992**, *441*, 185-195.

[59] Weidenbruch, M.; Ritschl, A.; Peters, K.; Schnering, H. G. v. Verbindungen des germaniums und zinns XI. Neue viergliedrige ringe: Thiatrigermetan, selenatrigermetan und N-phenyltrigermacyclobutanimin. *J. Organomet. Chem.*, **1992**, *438*, 39-44.

[60] Ohmori, Y.; Ichinohe, M.; Sekiguchi, A.; Cowley, M. J.; Huch, V.; Scheschkewitz, D. Functionalized Cyclic Disilenes via Ring Expansion of Cyclotrisilenes with Isocyanides. *Organometallics*, **2013**, *22*, 1591-1594.

[61] Adhikari, A. K., Sarosi, M. B., Grell, T., Lonnecke, P., Hey-Hawkins, E. Unusual Reactivity of Sodium Tetramesityltetraphosphanediide towards Cyclohexyl Isocyanide. *Chem. Eur. J.*, **2016**, *22*, 15664-15668.

[62] Streubel, R.; Ionescu, E.; Hoffman, N. Syntheses, structures, and reactions of new and novel four-, five and six-membered unsaturated N, P-heterocycle complexes. *Phosphorus, Sulfur, and Silicon*, **2004**, *179*, 809-811.

[63] Application of Trouton's rule assumes anisotropic solution phase conditions due to negligible intermolecular interactions and is usually reasonable in the absence of hydrogen bonding or other strong dipole interactions. The value of H_{vap} for ^iPrNC (31 kJ mol^{-1}) estimated under this assumption is in good agreement with experimentally determined values for other small alkyl isonitriles EtNC (33 kJ mol^{-1}) and MeNC (31 kJ mol^{-1}).[63] We also note that the estimated H_{vap} for EtNC calculated using Trouton's rule (boiling point = 77 °C for EtNC)[64] is 31 kJ mol^{-1}, which is only 6 % smaller than the experimental value of 33 kJ mol^{-1}.

[64] Feuer, H.; Rubinstein, H.; Nielson, A. T. Reaction of Alkyl Isocyanides with Ozone. A New Isocyanate Synthesis. *J. Org. Chem.*, **1958**, *23*, 1107-1109.

[65] Appel, R.; Paulen, W. Triphosphetanone, die ersten cyclischen Phosphaharnstoffderivate mit Vierring-Struktur. *Chem. Ber.*, **1983**, *116*, 2371-2373.

66 Frank, W.; Gelhausen, B.; Reiβ, G. J.; Salzer, R. Investigations on Systems of the Type PCl3/MCl3/Arene (M = Al, Ga), I. Reactions with Monohalobenzenes; Multinuclear NMR Spectroscopic Characterization of Aryldichlorohydrogenphosphonium Salts; Crystal Structure of para-Fluorophenyldichlorophosphonium Tetrachloroaluminate. *Z. Naturforsch.*, **1998**, *53B*, 1149-1168.

67 Resonances for this cation were assigned by comparison to NMR spectra of reaction mixtures containing isolated [(*dmap*)P(^{t}Bu)Cl][OTf], [**12Cl**][OTf], and excess NaF, which also showed signals at δ^{31}P = 199.5 ppm, δ^{19}F = -165.9 ppm, and $^1J_{PF}$ = 1066 Hz along with signals due to ^{t}BuPF$_2$. See Supporting Information for details.

68 [(*dmap*)$_2$P^{t}Bu][OTf]$_2$ was synthesized independently from a 1:2:2 mixture of ^{t}BuPCl$_2$, AgOTf, and *dmap* and characterized in situ. See experimental section for details.

69 Fritz, G.; Stoll, K. Reactions of Silylated Cyclotetraphosphanes with Lithium Alkyls. *Z. Anorg. Allg. Chem.*, **1986**, *539*, 65-86.

70 Schmidpeter, A.; Zirzow, K. Phosphinocyclopentadienide via Cyclopentadienylphosphide. *Z. Naturforsch.* **1987**, *42B*, 977-983.

71 Courtemanche, M-A.; Transue, W. J.; Cummins, C. C. Phosphinidene Reactivity of a Transient Vanadium P≡N Complex. *J. Am. Chem. Soc.*, DOI: 10.1021/jacs.6b10545.

72 Baudler, M.; Carlsohn, B.; Kloth, B.; Koch, D. Beiträge zur Chemie des Phosphors. 67. Zur Kenntnis der Cyclotriphosphane (PC$_6$H$_5$)$_3$, (PC$_6$H$_5$)$_2$(PC$_2$H$_5$) und (PC$_6$H$_5$)$_2$(PCH$_3$). *Z. Anorg. Allg. Chem.*, **1977**, *432*, 67-78.

73 Kostjuk, S. V. Recent progress in the Lewis acid co-initiated cationic polymerization of isobutylene and 1,3-dienes. *RSC Adv.*, **2015**, *5*, 13125-13144.

74 Analyzing the reaction mixture by ESI-MS showed the expected repeat unit of 80.06 m/z for the C$_6$H$_8$ monomer and signals corresponding to macromolecules containing up to 16 repeat units of cyclohexene (Figure S11, Supporting Information).

75 The identity of [**12Me**][OTf] was established by comparison of its ^{31}P NMR chemical shift (108.2 ppm) to that of [(*dmap*)PMe$_2$]$^+$ (91.3 ppm), by integration of the peaks in the ^{1}H NMR spectrum of [**12Me**][OTf], and by detection of a peak at 225.15 *m/z* for [**12Me**]$^+$ in a solution of [**7**][OTf] heated to 80 °C for 2 h.

76 Quin, L. D.; Caster, K. C.; Kisalus, J. C.; Mesch, K. A. Bridged ring systems containing phosphorus: structural influences on the stereochemistry of silane reductions of P-oxides and on carbon-13 and phosphorus-31 NMR properties of phosphines. *J. Am. Chem. Soc.*, **1984**, *106*, 7021-7032.

77 Krotokov, V. S.; Lorinov, O. V. Meijere, A. Ln(OTf)$_3$-Catalyzed Insertion of Aryl Isocyanides into the Cyclopropane Ring. *Synthesis*, **2006**, *21*, 3542-3546.

78 Bruker-AXS SAINT V8.27B Madison, Wisconsin.

79 G. M. Sheldrick, SADABS V2012/1, University of Göttingen, Germany.

80 Palatinus, L.; and Chapuis, G. SUPERFLIP a computer program for the solution of crystal structures by charge flipping in arbitrary dimensions *J. Appl. Crystallogr.*, **2007**, *40*, 786-790; Palatinus, L.; Prathapa, S. J.; van Smaalen, S. EDMA : a computer program for topological analysis of discrete electron densities. *J. Appl. Crystallogr.*, **2012**, *45*, 575-580.

81 Sheldrick, G. M. SHELXT: Integrated space-group and crystal-structure determination. *Acta Cryst.*, **2015**, *A71*, 3-8.

82 Sheldrick, G. M. A short history of SHELX. *Acta Crystallogr., Sect. A: Found. Crystallogr.*, **2008**, *64*, 112-122.

83 Dolomanov, O. V.; Bourhis, L. J.; Gildea, R. J.; Howard, J. A. K.; Puschmann, H., OLEX2: a complete structure solutions, refinement, and analysis program. *J. Appl. Crystallogr.*, **2009**, *42*, 339-341.

[84] Gaussian 09, Revision E.01, Frisch, M. J.; Trucks, G. W.; Schlegel, H. B.; Scuseria, G. E.; Robb, M. A.; Cheeseman, J. R.; Scalmani, G.; Barone, V.; Mennucci, B.; Petersson, G. A.; Nakatsuji, H.; Caricato, M.; Li, X.; Hratchian, H. P.; Izmaylov, A. F.; Bloino, J.; Zheng, G.; Sonnenberg, J. L.; Hada, M.; Ehara, M.; Toyota, K.; Fukuda, R.; Hasegawa, J.; Ishida, M.; Nakajima, T.; Honda, Y.; Kitao, O.; Nakai, H.; Vreven, T.; Montgomery, J. A., Jr.; Peralta, J. E.; Ogliaro, F.; Bearpark, M.; Heyd, J. J.; Brothers, E.; Kudin, K. N.; Staroverov, V. N.; Kobayashi, R.; Normand, J.; Raghavachari, K.; Rendell, A.; Burant, J. C.; Iyengar, S. S.; Tomasi, J.; Cossi, M.; Rega, N.; Millam, J. M.; Klene, M.; Knox, J. E.; Cross, J. B.; Bakken, V.; Adamo, C.; Jaramillo, J.; Gomperts, R.; Stratmann, R. E.; Yazyev, O.; Austin, A. J.; Cammi, R.; Pomelli, C.; Ochterski, J. W.; Martin, R. L.; Morokuma, K.; Zakrzewski, V. G.; Voth, G. A.; Salvador, P.; Dannenberg, J. J.; Dapprich, S.; Daniels, A. D.; Farkas, Ö.; Foresman, J. B.; Ortiz, J. V.; Cioslowski, J.; Fox, D. J. Gaussian, Inc., Wallingford CT, 2009.

For Table of Contents only:
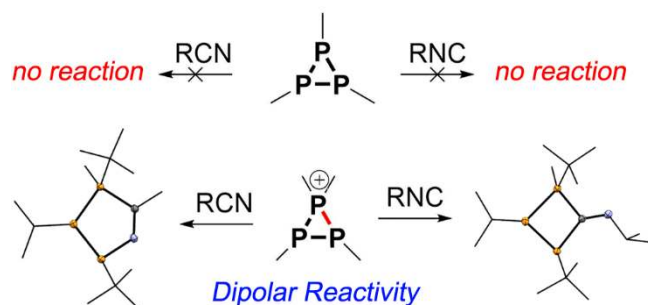
Synopsis: Ring strain and bond-polarization are both required for the addition of homoatomic P-P bonds to polar unsaturated substrates. The addition of P-P bonds to the $C\equiv N$ triple bond is reported along with the insertion of isonitriles to P-P bonds. These findings pave the way for the synthesis of new phosphorus containing ligands and provide broad insight into the chemistry of inorganic homocycles, including new strategies for activating nonpolar inorganic bonds.